

Expert-elicitation method for non-parametric joint priors using normalizing flows

Florence Bockting^{1*}, Stefan T. Radev² and Paul-Christian Bürkner¹

^{1*}Department of Statistics, TU Dortmund University, Vogelpothsweg 87, Dortmund, 44227, North Rhine-Westphalia, Germany.

²Cognitive Science Department, Rensselaer Polytechnic Institute, 110 Eighth Street, Troy, 12180, NY, United States.

*Corresponding author(s). E-mail(s): florence.bockting@tu-dortmund.de;
Contributing authors: stefan.radev93@gmail.com;
paul.buerkner@gmail.com;

Abstract

We propose an expert-elicitation method for learning non-parametric joint prior distributions using normalizing flows. Normalizing flows are a class of generative models that enable exact, single-step density evaluation and can capture complex density functions through specialized deep neural networks. Building on our previously introduced simulation-based framework, we adapt and extend the methodology to accommodate non-parametric joint priors. Our framework thus supports the development of elicitation methods for learning both parametric and non-parametric priors, as well as independent or joint priors for model parameters. To evaluate the performance of the proposed method, we perform four simulation studies and present an evaluation pipeline that incorporates diagnostics and additional evaluation tools to support decision-making at each stage of the elicitation process.

Keywords: prior elicitation, expert knowledge, joint prior distribution, normalizing flows, non-parametric priors

1 Introduction

The Bayesian paradigm offers the possibility to incorporate *prior knowledge* into a *statistical model* through the specification of *prior distributions*. This possibility is a central advantage of the Bayesian paradigm (Mikkola et al 2023), yet it also presents one of its most challenging aspects (Simpson et al 2017; Igorzata Roos et al 2015; Van Dongen 2006). In the following, we define prior knowledge as the expertise provided by a *domain expert* — an individual with extensive knowledge of a specific subject matter (Falconer et al 2022). This knowledge can be represented in various forms, but to integrate it into a Bayesian model, we need to translate it into a formal mathematical language that can be expressed as a prior distribution over the model parameters (Perepolkin et al 2023; O’Hagan 2019; Martin et al 2012; Garthwaite et al 2005).

A whole field of research, commonly referred to as (*expert*) *prior elicitation*, has emerged around the question of how to gather expert knowledge and translate it into appropriate prior distributions (Stefan et al 2022; Mikkola et al 2023; Falconer et al 2022). Garthwaite et al (2005) identified four key stages in a *prior elicitation process*:

1. **Setup stage:** In this stage, the problem is defined, an expert is selected, and the quantities to be elicited from the expert (referred to as *target quantities*) are determined;
2. **Elicitation stage:** Here, the target quantities are queried from the expert using specific elicitation techniques, resulting in what we call *elicited statistics*;
3. **Fitting stage:** This involves fitting a (potentially joint) probability distribution based on the expert-elicited statistics;
4. **Evaluation stage:** Finally, the adequacy of the fitted probability distribution is assessed in collaboration with the expert.

In this context, *elicitation methods* aim to provide a systematic and formal procedure for deriving prior distributions based on expert-elicited statistics. Early elicitation methods primarily tackled the problem by seeking analytical solutions, such as conjugate models or problem-specific transformation functions resulting in highly model-specific prior elicitation methods (see Mikkola et al 2023, for a recent review). This model dependence is partly due to the use of direct elicitation techniques, which involve asking experts directly about model parameters (Stefan et al 2022; Falconer et al 2022). This approach is problematic not only due to its inherent model dependence but also because model parameters are often challenging for domain experts to interpret meaningfully. Consequently, the quality of expert input can be questionable. In response to these limitations, substantial efforts have been made to develop methods that enable more flexible and interpretable prior specification for domain experts.

A recently proposed group of elicitation methods uses advances in machine learning to automate the process of translating expert knowledge into prior distributions (Hartmann et al 2020; da Silva et al 2019; Manderson and Goudie 2023; Bockting et al 2024). These methods address both key challenges: they allow expert knowledge to be expressed in terms of observable quantities and ensure that the elicited information remains interpretable for domain experts. Additionally, since the quantities elicited from the expert are not tied to specific model parameters, these methods are highly

versatile and model-independent. The underlying idea behind this approach is closely related to prior predictive checks, which are an integral part of the *Bayesian workflow* (Gelman et al 2020; Gabry et al 2019). The key concept is the *prior predictive distribution* (PPD), defined as $p(y) = \int p(y | \theta)p(\theta)d\theta$ with likelihood $p(y | \theta)$ and prior $p(\theta)$. The PPD establishes a formal relationship between the prior distributions of the model parameters and the model predictions, $p(y)$. In this way, the PPD provides a means to link expert knowledge, expressed in terms of observable quantities, to the latent model parameters. Since the PPD is often not analytically tractable, it is typically approximated using Monte Carlo integration (Mikkola et al 2023) which involves first sampling $\theta' \sim p(\theta)$ and then $y' \sim p(y | \theta')$. The resulting model predictions, y' , are then compared to expert knowledge on the outcome variable, y^* , using an appropriate discrepancy loss function. The goal is to learn prior distributions, $p(\theta)$, that produce model predictions consistent with expert knowledge by means of minimizing the discrepancy loss (Garthwaite et al 2005; Gelman et al 2017; Simpson et al 2017; Betancourt 2020).

The methods introduced so far that use this *simulation-based* approach focus on learning independent, parametric priors $p(\theta | \lambda)$, parameterized by a set of prior hyperparameters λ (Hartmann et al 2020; da Silva et al 2019; Manderson and Goudie 2023). While assuming *independent* priors for model parameters can be reasonable in some cases due to theoretical considerations or model constraints, this approach may not be sufficient for more complex or high-dimensional problems (Gelman et al 2017; 2020; Simpson et al 2017). In such cases, it becomes important to account for the *joint distribution* of model parameters to capture dependencies and interactions that reflect the underlying structure more accurately. Similarly, the use of *parametric* prior distribution families can be well-justified in some cases, but may lead to model misspecification in others, prompting the need for *non-parametric* approaches. Elicitation methods that focus on non-parametric priors are less studied, but examples include the use of Gaussian processes (Oakley and O’Hagan 2007) and quantile-parameterized distributions (Perepolkin et al 2023; 2024).

Building in particular on the work of Hartmann et al (2020); da Silva et al (2019); Manderson and Goudie (2023), we previously introduced a simulation-based framework with a highly modular structure that closely aligns with the elicitation process described by Garthwaite et al (2005). The advantage of this modular structure is its flexibility, allowing for easy adaptation to different types of methods. In our previous work (Bockting et al 2024), we demonstrated how to use this framework to learn parametric prior distributions for the model parameters. In this paper, we show how the same simulation-based framework can be used to learn flexible (i.e., non-parametric) joint priors for the model parameters with only minor adjustments to the workflow. In both approaches, we employ mini-batch stochastic gradient descent as the optimization method. However, our framework supports different optimization methods thanks to its modular design.

Main Contributions

Our motivation is two-fold: First, we aim to promote the development of a unifying, highly modular framework that supports a wide range of prior elicitation methods.

We believe that such a framework would benefit both users and developers of prior elicitation methods by providing structure and clarity in a field currently populated with numerous coexisting methods, which can make comparisons challenging. Second, we want to demonstrate how our simulation-based framework, introduced in [Bockting et al \(2024\)](#), can serve as a flexible approach for learning either parametric or non-parametric, as well as independent or joint, priors with only minor adjustments. While our previous work focused on learning parametric, independent priors, the present work emphasizes learning non-parametric, joint priors.

2 Methodology

In this paper, we propose an elicitation method that builds on and extends our recently introduced simulation-based framework ([Bockting et al 2024](#)). The overall idea of this framework closely resembles the approach of *prior predictive checks* ([Gelman et al 2020](#)): We simulate from the joint model $p(\theta, y)$ and assess how well the resulting prior predictions align with the expert’s expectations. If there is a discrepancy between the expert’s expectations and the simulations, the prior specification needs to be adjusted accordingly. [Figure 1](#) provides a graphical representation of the framework and [Table 1](#) offers a summary of the symbols and notation used in the following sections. The general workflow of our framework can be summarized as follows:

1. *Define the generative model*: Define the generative model including dimensionality and parameterization of prior distribution(s). (Setup stage; [Section 2.1](#))
2. *Identify variables and elicitation techniques for querying expert knowledge*: Select the set of variables to be elicited from the domain expert (target quantities) and determine which elicitation techniques to use for querying the selected variables from the expert (elicited statistics). (Setup stage; [Section 2.2](#))
3. *Elicit statistics from expert and simulate corresponding predictions from the generative model*: Sample from the generative model and perform all necessary computational steps to generate model predictions (model-elicited statistics) corresponding to the set of expert-elicited statistics. (Elicitation stage; [Section 2.3](#))
4. *Evaluate consistency between expert knowledge and model predictions*: Evaluate the discrepancy between the model- and expert-elicited statistics via a multi-objective loss function. (Fitting stage; [Section 2.4](#))
5. *Adjust prior to align model predictions more closely with expert knowledge*: Use mini-batch stochastic gradient descent to adjust the prior so as to reduce the loss. (Fitting stage; [Section 2.4](#))
6. *Find prior that minimizes the discrepancy between expert knowledge and model predictions*: Repeat steps 2 to 5 iteratively until a prior is found that minimizes the discrepancy between the model and expert-elicited statistics. (Fitting stage; [Section 2.4](#))
7. *Evaluate the learned prior distributions*: Run the learning algorithm (steps 2 to 6) multiple times to obtain a set of prior distributions that can equally well represent the expert data. Select a plausible prior distribution in consultation with the domain expert or apply model averaging techniques. (Evaluation stage; [Section 2.5](#))

The following sections discuss each step in greater detail.

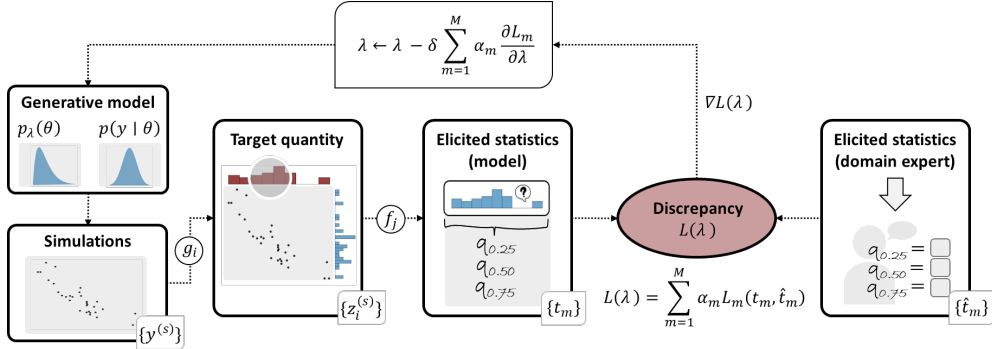


Fig. 1 Graphical illustration of our simulation-based prior-elicitation framework. The process begins by identifying target quantities to be elicited from the domain expert and selecting appropriate elicitation techniques, which result in (expert-)elicited statistics. Next, predictions are simulated from the generative model by sampling from the prior $p_\lambda(\theta)$ and computing the corresponding model-implied target quantities and elicited statistics. The consistency between model- and expert-elicited statistics is assessed using a loss function L_m , where α_m is the weight of the m^{th} loss component. Hyperparameters λ that define the learned prior are adjusted based on this evaluation to reduce the loss and align model predictions more closely with expert knowledge. This iterative process continues until a prior is found that minimizes the discrepancy between model and expert-elicited statistics. In the updating rule, δ refers to the step size.

2.1 Prior Specification & Learning

In our previous work (Bockting et al 2024), we introduced the simulation-based framework along with a method for learning a set of *independent parametric* prior distributions, $p(\theta_k | \lambda_k)$, for the model parameters θ_k with $k = 1, \dots, K$. In this paper, we extend our framework by introducing a method to learn a *joint non-parametric* prior distribution $p_\lambda(\theta) = p_\lambda(\theta_1, \dots, \theta_K)$ over all model parameters θ . In both the parametric and non-parametric approaches, the objective of the optimization process is to learn the hyperparameters λ that minimizes the discrepancy between the model simulations and the expert expectations. However, the interpretation of these hyperparameters differs between approaches, which we emphasize by using a different notation for the prior distributions. In the non-parametric approach, we employ *normalizing flows* (NFs) to induce a flexible family of prior distributions which entail specialized deep neural networks with trainable parameters λ (Kobyzev et al 2020). Thus, in the non-parametric approach, λ represents the weights of the deep neural networks within the NFs, whereas in the parametric approach, λ denotes the parameters of the associated prior distribution families (i.e., the prior hyperparameters).

Normalizing Flows

To learn a non-parametric joint prior for the model parameters, we use normalizing flows (NFs), a family of deep generative models that offers tractable density evaluation

| <i>Symbol</i> | <i>Description</i> |
|--|---|
| <hr/> Simulation-based prior elicitation <hr/> | |
| y_n | data $n = 1, \dots, N$ |
| θ_k | model parameter $k = 1, \dots, K$ |
| λ | model hyperparameter |
| $p(y \theta)$ | likelihood |
| $p(\theta \lambda)$ | prior parameterized by λ |
| $p(y)$ | prior predictive distribution |
| $z_i = c_i(\lambda)$ | simulated model target quantity defined by function c_i |
| \hat{z}_i | expert representation of the target quantity |
| $t_m = f_j(z_i)$ | model-elicited statistic defined by elicitation technique f_j |
| \hat{t}_m | expert-elicited statistic |
| $L_m(t_m(\lambda), \hat{t}_m)$ | loss component |
| $L(\lambda) = \sum_{m=1}^M \alpha_m L_m(t_m(\lambda), \hat{t}_m)$ | total loss as weighted sum of L_m with weights α_m |
| $p_{\lambda_1, \dots, \lambda_R}(\theta) = \sum_{r=1}^R w_r \cdot p_{\lambda_r}(\theta)$ | averaged prior across R replications and weighted by w_r with $r = 1, \dots, R$ |
| $\Delta_r(L) = L(\lambda_r) - L(\lambda_{\min})$ | difference between total loss of replication r and replication with minimum total loss |
| $w_r = \frac{\exp\{-\gamma \Delta_r(L)\}}{\sum_{v=1}^V \exp\{-\gamma \Delta_v(L)\}}$ | weights used for model averaging with γ being a scaling factor; in all simulation studies $\gamma = 1$. |
| <hr/> Normalizing flow <hr/> | |
| $u \sim p_U(u)$ | samples from base distribution |
| $g_\lambda(\cdot)$ | generator function |
| $u = g_\lambda(\theta)$ | normalizing direction |
| $\theta = g_\lambda^{-1}(u)$ | generative direction |
| $g_\lambda = g_{\lambda_H} \circ \dots \circ g_{\lambda_1}$ | composition of H coupling layers |

Table 1 Notation and symbols used in this paper.

(Kobyzev et al 2020). NFs transform a simple probability distribution, the *base distribution* $p(u)$, into a complex *target distribution* — in our case, the joint prior $p_\lambda(\theta)$ — through a series of invertible and differentiable mappings g_λ , parameterized by λ (Kobyzev et al 2020). The composition of invertible functions g_λ yields an explicit form of the density $p_\lambda(\theta)$ via the change of variables formula

$$p_\lambda(\theta) = p(u = g_\lambda(\theta)) | \det g'_\lambda(\theta) |,$$

where $g'_\lambda(\theta) = \frac{\partial}{\partial \theta} g_\lambda(\theta)$ is the Jacobian matrix of g_λ at θ and $| \det g'_\lambda(\theta) |$ is its absolute determinant. This formula allows us to easily evaluate the prior density at arbitrary points of interest θ (Dinh et al 2016). Obtaining samples from the joint prior can be achieved by first sampling from the base distribution, $p(u)$, and then applying the inverse $g_\lambda^{-1}(u)$ to obtain samples from $p_\lambda(\theta)$:

$$\theta = g_\lambda^{-1}(u) \sim p_\lambda(\theta) \quad \text{for } u \sim p(u).$$

Typically, $p(u)$ is chosen to be a simple density, such as a standard Gaussian or a uniform distribution (Kobyzev et al 2020). Figure 2 depicts the use of NFs for learning a non-parametric prior distribution within our simulation-based framework.

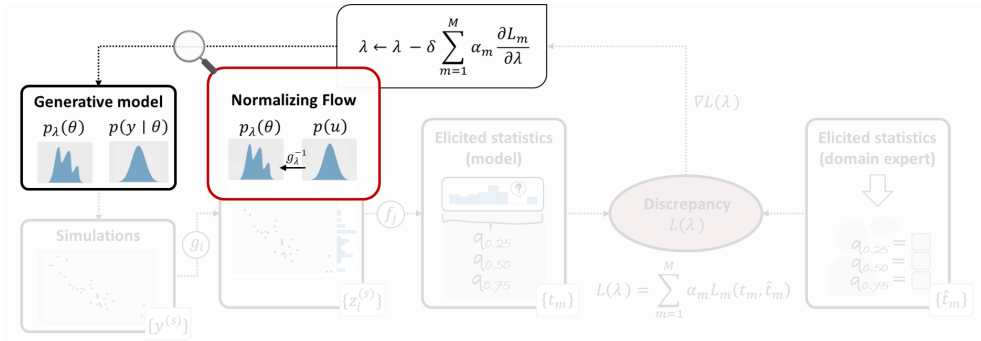


Fig. 2 Learning non-parametric prior distributions using normalizing flows within our simulation-based framework. Normalizing flows transform a simple probability distribution, the *base distribution* $p(u)$, into a complex *target distribution* — in our case, the joint prior $p_\lambda(\theta)$ — through a series of invertible and differentiable mappings g_λ , parameterized by λ .

For NFs to be practical, the mapping g_λ should be easily invertible, computationally efficient, and sufficiently expressive to model any target distribution of interest (Kobyzev et al 2020). Several types of NFs that meet these requirements have been proposed, including affine (Dinh et al 2014) and spline coupling flows (Durkan et al 2019). A detailed discussion and introduction to coupling flows can be found in various sources (Draxler et al 2024; Dinh et al 2014; 2016; Radev et al 2020; Kobyzev et al 2020; Papamakarios et al 2021; Bond-Taylor et al 2021). Due to their simple architecture, affine coupling flows are easy to invert and computationally efficient, although they have restricted expressiveness (Bond-Taylor et al 2021). However, the expressiveness of a coupling flow can be increased by stacking multiple affine coupling layers, $g_\lambda = g_{\lambda_H} \circ \dots \circ g_{\lambda_1}$ with $h = 1, \dots, H$ coupling blocks (Dinh et al 2016). In fact, Draxler et al (2024) prove that affine coupling flows are distributional universal approximators, capable of representing any target distribution despite their seemingly restrictive architecture. In line with these considerations and the strong empirical performance of affine coupling flows, we focused on this type of normalizing flows in our simulation studies (see Section 4), using the implementation provided by BayesFlow (Radev et al 2023).

Finally, it is worth noting that, since our focus is solely on the mapping from the base distribution to the target distribution (i.e., the generative direction of NFs), virtually any other generative model family could be used to learn how to generate samples from a joint prior. Examples of common generative architecture alternatives include diffusion models (Cao et al 2024) and flow matching (Lipman et al 2022). However, we used NFs here because they perform well in practice and are computationally efficient. In particular, they do not require solving differential equations during sampling (Draxler et al 2024).

2.2 Target Quantities & Elicitation Techniques

A key task in the setup stage of the elicitation process is the selection of target quantities and elicitation techniques to effectively gather the expert information. Two

main criteria should guide this selection: *interpretability* and *informativeness* (Mikkola et al 2023; Crowder 1992; da Silva et al 2019; Garthwaite et al 2005).

Selecting Target Quantities

Interpretability refers to the selection of target quantities that allows domain experts to meaningfully express their knowledge based on their experience and expertise (Garthwaite et al 2013). Target quantities on the same scale as the outcome variable (cf., *observable* quantities) are considered to be highly interpretable (da Silva et al 2019; Manderson and Goudie 2023). In contrast, target quantities that refer to model parameters are more challenging to interpret, especially when the outcome variable is not on the same scale as the model parameters (Kadane and Wolfson 1998; Kadane et al 1980). Therefore, it is sometimes advocated asking experts exclusively about observable quantities (Kadane and Wolfson 1998). We share the view of Denham and Mengersen (2007) that the appropriateness of either approach depends on the specific problem being addressed and the type of expert providing the information.

Guided by this idea, we define a target quantity in our framework in the most general sense as a function of the trainable hyperparameters of the prior: $z_i = c_i(\lambda)$. If we want to elicit the expert’s knowledge regarding the outcome variable, we obtain the target quantity by defining the function c_i as a query to the prior predictive distribution $p(y) = \int p(y | \theta)p_\lambda(\theta)d\theta$, marginalizing the likelihood over the prior: $z_i = c_i(\lambda) \equiv y$. Here, z_i refers to the distribution of an observable quantity. However, if we want to elicit expert knowledge about a model parameter θ_k , for instance, available due to previous experiments or results from meta-analyses, we define c_i as a simple projection on θ_k : $z_i = c_i(\lambda) \equiv \theta_k$. In this case, z_i refers to the distribution of a model parameter. In this way, we can also accommodate any other target quantity that can be derived from the model parameters or the data (e.g., R^2 ; the proportion of variance explained by the model; Gelman et al 2019).

Selecting Elicitation Techniques

Once the set of target quantities has been selected, we need to determine how to elicit this information from the expert, which requires choosing an appropriate *elicitation technique*. While experts can be asked to provide the full distribution of a target quantity (e.g., in the form of a histogram (Johnson et al 2010)), another common technique is to focus on specific summary statistics (Morris et al 2014). Research on prior elicitation suggests that experts can reasonably be asked to describe a target quantity using proportions, the mode, the median, and generally quantiles (Garthwaite et al 2005; Stefan et al 2022; O’Hagan et al 2006), with quantile-based elicitation techniques being particularly recommended (Kadane and Wolfson 1998). In contrast, asking about the mean is less advisable when the distribution is skewed (Peterson and Miller 1964), and similarly, querying variances is in general discouraged (Garthwaite et al 2005; Kadane and Wolfson 1998). Furthermore, assessing dependencies between variables is challenging, making the elicitation of joint priors especially difficult (Garthwaite et al 2005). Elicitation of correlations in the context of joint priors has been studied among others by Gokhale and Press (1982); Clemen et al (2000), and Dickey et al (1985) as reviewed by Mikkola et al (2023).

In our elicitation method, we represent an elicitation technique as a function f_j of a target quantity z_i . The resulting set of *elicited* target quantities is referred to as *elicited statistics*, $\{t_m(\lambda)\}$, where $t_m(\lambda) = f_j(z_i)$ and m refers to the corresponding $i \times j$ combination. In the following, we sometimes keep the dependency on λ implicit and simply write t_m instead of $t_m(\lambda)$.

Sensitivity Analysis

In addition to interpretability, the second criterion for selecting target quantities and elicitation techniques is *informativeness*, which refers to the relevance of the elicited statistics for learning the prior distributions. Evaluating this criterion is nontrivial because the relationship between the elicited statistics and the model (hyper-)parameters is complex and often analytically intractable. One computational approach to assess informativeness is to conduct a *sensitivity analysis* (Depaoli et al 2020). In this approach, we systematically vary one aspect of the prior distribution at a time while keeping all other aspects constant. For each specific change in the prior, we run the generative model in forward mode by sampling from the prior, then from the likelihood, and subsequently computing the target quantities and elicited statistics. Sensitivity analysis enables us to assess how changes in one aspect of the prior distribution impact each elicited statistic. If we observe no variation in a particular elicited statistic for a given prior variation, this statistic does not provide any useful information for the learning algorithm to determine the corresponding aspect of the prior. This approach can help inform the selection of elicited statistics and identify which aspects of the prior are most likely to remain unidentifiable given the current set of expert information.

2.3 Model-implied & Expert-elicited Statistics

After determining the set of target quantities and corresponding elicitation techniques, we can proceed to gather information from the expert through specific *prior elicitation protocols* (Gosling 2018; Cooke 1991; Authority 2014). This process may be preceded by a training phase to familiarize the expert with the elicitation tasks (Stefan et al 2022). In prior elicitation research, an entire subfield has focused on determining how to conduct optimal expert interviews, taking into account factors such as cognitive biases and heuristics. While it is beyond the scope of this paper to review this literature, several comprehensive reviews are available (e.g., Mikkola et al 2023; Stefan et al 2022; Falconer et al 2022). At this point, we will skip the actual interrogation process and assume that the expert information has been successfully gathered, providing us with a set of expert-elicited statistics, denoted by \hat{t}_m .

Given the set of expert-elicited statistics, $\{\hat{t}_m\}$, we can evaluate the discrepancy between the expert expectations and the model-implied statistics, $\{t_m\}$. The latter are computed by simulating from the model. This proceeds as follows: We start with an arbitrary initial prior distribution from which we sample model parameters $\theta^{(s)} \sim p_{\lambda_0}(\theta)$, where λ_0 represent the initial hyperparameter values that define the prior distribution. The superscript s denotes the s^{th} sample out of a total of S samples. Subsequently, we perform all necessary computational steps to derive samples from

the target quantities $z_i^{(s)}$. Finally, we apply the corresponding elicitation technique to obtain the model-implied statistics $t_m = f_j(\{z_i^{(s)}\})$ from the simulations.

As an example, consider a Binomial regression model with a dummy-coded categorical predictor x with two levels and model parameters $\theta = (\theta_1, \theta_2)$ representing the intercept and slope. We decide to query the expert about the quartiles of the expected outcome variable y conditional on each group, gr_1 and gr_2 . That is, we obtain six expert-elicited statistics $Q_p(y_{\text{gr}_i})$ with $p = 0.25, 0.50, 0.75$ and $i = 1, 2$. To obtain the corresponding model-implied statistics, we would first sample the model parameters from the initial prior distribution, $\theta^{(s)} \sim p_{\lambda_0}(\theta)$ and compute the linear predictor $\eta_{\text{gr}_i}^{(s)} = \theta_1^{(s)} + \theta_2^{(s)} x_i$ transformed by an inverse-link function σ to obtain the implied event probabilities $p_{\text{gr}_i}^{(s)} = \sigma(\eta_{\text{gr}_i}^{(s)})$. Then we would sample from the likelihood providing us with samples from the implied prior predictive distribution, $y_{\text{gr}_i}^{(s)} \sim \text{Binomial}(p_{\text{gr}_i}^{(s)}, N)$. We repeat this sampling process S times resulting in sets $\{y_{\text{gr}_i}^{(s)}\}$ of S samples. Finally, we compute the quartiles from these samples, resulting in the six model-implied statistics $Q_p(\{y_{\text{gr}_i}^{(s)}\})$ with $p = 0.25, 0.50, 0.75$ and $i = 1, 2$.

2.4 Discrepancy Evaluation & Training

To evaluate the discrepancy between the model- and expert-elicited statistics, an appropriate loss function is used for each statistic, $L_m(t_m(\lambda), \hat{t}_m)$. Different loss functions may be preferable depending on the type of the respective elicited statistic. Since the discrepancy is computed for each statistic within the set of elicited statistics, the total loss comprises multiple *loss components*, which are combined into a single total loss using a weighted sum:

$$L(\lambda) = \sum_{m=1}^M \alpha_m L_m(t_m(\lambda), \hat{t}_m), \quad (1)$$

where α_m denote the weights. The choice of weights α_m can be guided by different considerations: One approach is to manually adjust the weights based on the importance of the individual loss components from the expert’s perspective (Wang et al 2011). Alternatively, automated weighting methods, known as loss-balancing methods, can be used to optimally balance the contribution of each individual term to the total gradient (Liu et al 2019; Crawshaw 2020; Bischof and Kraus 2021).

After computing the total loss, $L(\lambda)$, the gradients with respect to the hyperparameters λ are calculated. These gradients are then used to adjust the hyperparameters in the opposite direction:

$$\lambda' \leftarrow \lambda - \delta \sum_{m=1}^M \alpha_m \frac{\partial L_m}{\partial \lambda}, \quad (2)$$

with δ being the step size (Goodfellow et al 2016). We employ mini-batch stochastic gradient descent (SGD) with automatic differentiation, facilitated by the (explicit or implicit) reparameterization trick (Kingma and Welling 2014; Figurnov et al 2018). With the adjusted hyperparameters λ' , new samples from the prior $p_{\lambda'}(\theta)$ can be generated and the updated model-implied statistics $t_m(\lambda')$ computed. We then reassess

the discrepancy between the model-implied and expert-elicited statistics and continue to adjust the hyperparameters as needed. This iterative process continues until a convergence criterion is met or a stopping rule is applied.

2.5 Evaluation of Training Results

Convergence Checks

Training is considered successful if the loss is minimized and no further learning occurs. With a proper discrepancy measure as loss function, it is guaranteed that the total loss (and the individual loss components) approach zero as learning progresses. The learning progress can be tracked by examining the loss behavior across epochs, where a decreasing trend is expected until the loss stabilizes at a value close to zero. Further insights into the learning progress can be obtained by tracking the convergence of additional quantities of interest beside the loss, for instance the mean and standard deviation of the marginal priors.

A further method to assist in the examination of convergence is to compute the slope of a linear regression fitted to the loss values over the last m epochs, whereby m should not be taken too large such that the linearity assumption holds. Typically, the overall loss function exhibits exponential decay, but once the loss stabilizes, a linear trend is a good approximation. Ideally, a slope of zero would indicate perfect convergence, though some variation is expected in practice. To evaluate whether the slope remains acceptable, the training algorithm can be run repeatedly with random seeds and the absolute slopes across all replications can be compared. For training runs with the highest final slopes, we can perform a visual inspection of the trajectories of key quantities across epochs, such as the total loss, loss components, and prior means and standard deviations. If these runs show successful convergence, we can reasonably conclude that other runs (with smaller final slopes) have also converged.

Non-uniqueness of Learned Priors

Once the elicited statistics have been learned accurately, we can examine the learned prior distribution that corresponds to this set of expert-elicited statistics. However, there are often multiple optimal values λ^* that align closely with the elicited statistics yet result in different prior distributions (da Silva et al 2019; Manderson and Goudie 2023; Stefan et al 2022). This lack of uniqueness is anticipated, given the limited information provided by the set of elicited statistics compared to the complexity of the generative model (Manderson and Goudie 2023). Furthermore, when target quantities refer solely to the observable space, we only gain access to the model’s overall uncertainty with limited ability to differentiate between aleatoric and epistemic uncertainty (Nemani et al 2023; Perepolkin et al 2024). Aleatoric uncertainty, by definition, is irreducible; however, several methods exist to reduce epistemic uncertainty. These include (i) selecting more informative target quantities, (ii) eliciting more detailed expert information (e.g., increasing the number of quantiles in quantile-based elicitation), (iii) adding theory-informed regularization terms to constrain the search space (as illustrated in Manderson and Goudie 2023), (iv) improving the initialization

method to achieve better starting points, and (v) employing more advanced optimization algorithms when dealing with a large number of model parameters (Nemani et al 2023).

Model Averaging

Given the (potential) non-uniqueness of the learned prior distributions, it is advisable to run the training multiple times on the same expert data but with different random seeds. This approach helps provide insight into the variability among the learned prior distributions. From the resulting set of candidate priors $p_{\lambda_r}(\theta)$ for $r = 1, \dots, R$, we can, in consultation with the domain expert, exclude prior distributions that do not meet the expert’s expectations. For the remaining set of prior distributions, which may be considered practically equivalent from the expert’s perspective, either a single prior distribution can be chosen, or alternatively, model averaging techniques can be applied. In the case of model averaging, the combined prior would take the form:

$$p_{\lambda_1, \dots, \lambda_R}(\theta) = \sum_{r=1}^R w_r \cdot p_{\lambda_r}(\theta) \quad (3)$$

where the weights w_r sum to one. The weights w_r can either be assigned by the user, based on theoretical assumptions, or selected according to one of several proposed weighting schemes (Claeskens and Hjort 2008). Here, we apply an approach suggested by Buckland et al (1997) for the general purpose of model averaging and selection, where the weights w_r are defined as

$$w_r = \frac{\exp\{-\gamma I_r\}}{\sum_{v=1}^V \exp\{-\gamma I_v\}}.$$

In the above expression, γ is a scaling factor, and I represents the performance criterion by which the models are weighted. This definition ensures that models with identical performance receive equal weight (Buckland et al 1997). In our setting, it is sensible to use the total loss $L(\lambda_r)$ of each replication r as the performance criterion. Consequently, the “best” model is the one with the smallest total loss, $L(\lambda_{\min})$ (Bissiri et al 2016). This yields the following definition of weights

$$w_r = \frac{\exp\{-\gamma \Delta_r(L)\}}{\sum_{v=1}^V \exp\{-\gamma \Delta_v(L)\}}. \quad (4)$$

where $\Delta_r(L) = L(\lambda_r) - L(\lambda_{\min})$. The difference is used primarily for computational reasons to ensure numerical stability (Claeskens and Hjort 2008). The formulation in Eq. (4) can be interpreted as the probability of replication r representing the best prior, given the collection of learned prior distributions (Wagenmakers and Farrell 2004). The scaling factor γ controls the influence of each replication’s relative performance $\Delta_r(L)$. When $\gamma > 1$, discrepancies in model performance are amplified, with better models receiving higher weights and worse models receiving lower weights. As $\gamma \rightarrow \infty$, this weighting would approach a one-hot vector, effectively performing model selection.

Conversely, when $\gamma < 1$, the performance differences between models are smoothed out, reducing the influence of performance discrepancies.

Simulating From an “Oracle”

The simulation-based framework enables us to evaluate the degree of non-identifiability and determine if further regularization is required, even before querying any data from the expert. An effective approach involves using an *oracle*, where a pre-defined prior distribution serves as the *ground truth*. From this “true” prior, we perform forward simulations: sampling first from the prior, then from the likelihood, and carrying out all necessary computational steps to generate a set of model-implied statistics corresponding to the ground truth. This set of simulated statistics can then serve as a proxy for the “expert-elicited” statistics.

Using the above approach allows us to assess the self-consistency of the algorithm, the degree of non-identifiability (i.e., how informative are the elicited statistics), and the suitability of the chosen algorithm parameters used for training NFs with mini-batch SGD. Additionally, we can use this ground truth as a benchmark to assess whether the learned prior distributions approximate it reasonably well, even though non-identifiability may prevent us from exactly recovering the underlying “true” prior distribution.

3 Implementation

In all simulation studies, we use a batch size of 128. To simulate from an oracle (discussed in Section 4.1), we draw once $S = 10,000$ samples from the true joint prior and then compute the corresponding set of “expert”-elicited statistics. During training with mini-batch SGD we draw $S = 200$ samples from the joint prior. To evaluate the discrepancy between the model-implied and expert-elicited statistics, we use a biased *Maximum Mean Discrepancy* (MMD) loss with an energy kernel (Gretton et al 2006; Feydy et al 2019), following our previous success with the metric (Bockting et al 2024). For the correlation between parameters, however, we apply a squared-error loss (for details see Section 4.1). The total loss is computed as a weighted sum of the individual loss components, with unit weights assigned to the MMD loss components and a weight of 0.1 applied to the squared-error loss components.

The architecture of the NFs is rather simple compared to typical applications in deep learning (e.g., Kingma and Dhariwal 2018) and consists of a standard multivariate Gaussian as a base distribution and three affine coupling blocks. Each coupling block consists of two dense layers with 128 units and ReLU activation functions. In Simulation Study 1, the number of learnable hyperparameters is $|\lambda| = 202,776$, while in the case studies corresponding to Simulation Study 2, it is $|\lambda| = 205,872$. In Simulation Study 1, we assume a discrete likelihood and use the softmax-gumble trick to compute the gradients of a discrete random variable (for more information, see Bockting et al 2024). The gradients of the total loss with respect to the hyperparameters are used to update the hyperparameters λ . Optimization was performed with the Adam optimizer for 600 epochs in Simulation Study 1 and 1500 epochs in Simulation Study 2. We used a fixed learning rate of 0.00025 for Simulation Study 2,

Scenario 1 & 2, and 0.0001 for Simulation Study 1 and Stimulation Study 2, Scenario 3. These algorithm (hyper-)parameter values were obtained by manual tuning until good performance across all of our case studies was achieved.

All simulations were implemented in Python 3.11.10 using the following libraries: TensorFlow 2.14 (Abadi et al 2016), TensorFlow Probability 0.22.1 (Dillon et al 2017), NumPy 1.24.3 (Harris et al 2020), pandas 2.2.3 (McKinney et al 2010), and BayesFlow 1.1.6 (Radev et al 2023). Simulations were run on the Linux HPC cluster at Technical University Dortmund (LiDO3) on high-end CPUs.

4 Simulation Studies

4.1 General Setup

In the following, we present four case studies organized across two simulation studies to evaluate the performance of our elicitation method. In Simulation Study 1, we introduce a simple Binomial regression model with one continuous predictor. In Simulation Study 2, we present three scenarios based on a normal regression model with a three-level categorical predictor, differing only in the pre-defined joint prior representing the ground truth. Table 2 provides an overview of the generative models and the ground truth joint priors (discussed next) used in the upcoming simulation studies. Before introducing the simulation studies, we will discuss the decisions made in the simulation setup in greater detail. The implementation and simulation results can be found on GitHub (https://github.com/florence-bockting/prior_elicitation/tree/main/elicit/manuscript_non_parametric_joint_prior) and OSF (<https://osf.io/xrzh6/>), respectively. Information about the training time for each simulation study is provided in Appendix A.1.

Simulated Expert as Ground Truth

For the simulation studies in this paper, we simulate expert input using synthetic data generated from a predefined joint prior representing the ground truth (i.e., oracle, see Section 2.5 for details). For simplicity, we use a parametric prior with fixed hyperparameter values as ground truth for each case study. Further details on the exact specification of the “true” joint prior is provided in the respective case-study sections and in Table 2.

Selection of Target Quantities and Elicitation Techniques

Following recommendations in the field, we focused on observable quantities when selecting target quantities for our simulation studies (see Section 2.2 for details). For the Binomial regression model, we used the expected observations of the outcome variable conditional on two observations of the continuous predictor, $y \mid x_0$ and $y \mid x_1$. For the normal regression model, we considered the prior predictive observations conditional on the three groups, $y \mid gr_i$ for $i = 1, 2, 3$.

However, we had to deviate from the recommendation to select observable target quantities in two respects. First, we included R^2 as an additional target quantity for the normal model (Simulation Study 2), motivated by the following reasoning: if

| <i>Model</i> | <i>Generative Model</i> | <i>Ground Truth</i> |
|---|--|--|
| Binomial — M1 (Section 4.2) | $y_i \sim \text{Binomial}(p_i, 30)$ $p_i = \text{sigmoid}(\beta_0 + \beta_1 x_i)$ | $\beta_0 \sim \text{Normal}(0.1, 0.1)$ $\beta_1 \sim \text{Normal}(-0.1, 0.3)$ |
| Normal models | | |
| <i>Scenario 1</i> — M2 (Section 4.3.1) | $y_i \sim \text{Normal}(\mu_i, \sigma)$ $\mu_i = \beta_0 + \beta_1 x_{1,i} + \beta_2 x_{2,i}$ | $\beta_0 \sim \text{Normal}(10, 2.5)$ $\beta_1 \sim \text{Normal}(7, 1.3)$ $\beta_2 \sim \text{Normal}(2.5, 0.8)$ $\sigma \sim \text{Gamma}(5, 2)$ |
| <i>Scenario 2</i> — M3 (Section 4.3.2) | see M2 | $\beta_0 \sim \text{Normal}(10, 2.5)$ $\beta_1 \sim \text{SkewNormal}(7, 1.3, 4)$ $\beta_2 \sim \text{SkewNormal}(2.5, 0.8, 4)$ $\sigma \sim \text{Gamma}(5, 2)$ |
| <i>Scenario 3</i> — M4 (Section 4.3.3) | see M2 | $\beta \sim \text{Mv-Normal}\left(\begin{bmatrix} 10 \\ 7 \\ 2.5 \end{bmatrix}, D(s) \mathbf{R} D(s)\right)$ $\mathbf{R} = \begin{bmatrix} 1. & 0.3 & -0.3 \\ 0.3 & 1. & -0.2 \\ -0.3 & -0.2 & 1. \end{bmatrix}$ $s = (2.5, 1.3, 0.8)$ $\sigma \sim \text{Gamma}(5, 2)$ |

Table 2 Overview of generative models and ground truth in the simulation studies. Symbols: \mathbf{R} denotes the correlation matrix and s the vector of standard deviations.

we only have information about the outcome variable for each of the three groups, we provide the learning algorithm with no means to differentiate between parameter uncertainty and data uncertainty. The coefficient of determination, R^2 , represents the ratio of parameter uncertainty to total uncertainty (which encompasses both data and parameter uncertainty). Consequently, it offers more information for the learning algorithm to differentiate between these two types of uncertainty, even though it may be somewhat more challenging for a domain expert to interpret. However, as R^2 is commonly reported as a metric in a regression context, we would argue that this quantity is still well understood by domain experts.

Second, we included the pairwise correlation between model parameters in the set of target quantities for each case study. If independence between model parameters is assumed, all correlations are set to zero; otherwise, we use the exact correlation structure indicated by the ground truth. We acknowledge that this information cannot be reasonably demanded from a domain expert in most cases. However, we currently lack suitable elicitation methods for asking domain experts about interpretable quantities that provide sufficient information regarding the correlation structure between the model parameters. A future task will be to develop such elicitation methods and to then incorporate these methods into our computational framework.

Regarding the selection of *elicitation techniques*, we follow the recommendation to query quantiles from a domain expert (Kadane and Wolfson 1998). For each target quantity, except for the correlation information, we elicit five quantiles: 5%, 25%, 50%, 75%, 95%. For the correlation values, we assume that the expert provides a single point estimate corresponding to a moment-based elicitation approach. To

assess whether the selected set of elicited statistics is sufficiently informative to determine a prior distribution for the model parameters, we conduct a *sensitivity analysis* for each case study.

Evaluation of Simulation Results

We run each simulation study 30 times with different random seeds. For each replication, we calculate the slope of the loss trajectory over the last 100 epochs and perform a visual convergence check for the five replications with the highest absolute slopes (i.e., worst cases). In this visual check, we examine the trajectories of the total loss, the loss components related to the elicited statistics, and the mean and standard deviation for each marginal prior across epochs. If this visual inspection indicates satisfactory convergence, we consider the convergence of all other replications to be successful as well. Additionally, we check the match between the final model-implied and expert-elicited statistics. Finally, we examine the learned prior distributions for each replication and compute the model average across the 30 learned prior distributions.

Summary of Analysis Workflow

Table 3 provides a summary of the analysis workflow followed in each of the subsequent simulation studies.

4.2 Simulation Study 1: Binomial Likelihood with Independent Normal Priors

We introduce the general idea of our method using a Binomial model with a logit link (sigmoid response function) and one continuous predictor $x = 1, \dots, 50$, scaled by its standard deviation. In the following we refer to this model as [M1](#):

$$\begin{aligned} y_i &\sim \text{Binomial}(p_i, 30) \\ p_i &= \text{sigmoid}(\beta_0 + \beta_1 x_i) \\ \beta_0, \beta_1 &\sim p_\lambda(\beta_0, \beta_1) \\ \theta &\equiv (\beta_0, \beta_1) \end{aligned} \tag{M1}$$

The goal is to learn a joint prior for the model parameters β_0 (intercept) and β_1 (slope), assuming independence between these parameters.

Setup & Elicitation Stage

As elicited statistics, we select two observations from the continuous predictor x , denoted by x_0 and x_1 , which correspond to the 25% and 75% quantiles of x_i . We select specific quantiles rather than randomly sampling two observations from the predictor to avoid the observations being too close together, which would reduce informativeness. From the two selected observations, we compute five quantiles from the prior predictive distribution to represent the elicited statistics (see Section 4.1 for details). To obtain the “expert”-elicited statistics, we define a true prior that represents the ground truth and simulate from the generative model in forward mode,

| <i>Task</i> | <i>Approach</i> | <i>Insights</i> |
|---|--|--|
| Setup & Elicitation Stage | | |
| Select the set of elicited statistics and evaluate its informativeness. | (1) Simulate elicited statistics by defining a true joint prior (i.e., the oracle). (2) Conduct a sensitivity analysis. | Can the set of elicited statistics provide sufficient information to learn the key aspects of the joint prior? |
| Fitting Stage | | |
| Evaluate variability in learned priors to assess non-identifiability. | Run the training algorithm several times with different random seeds. | Do different training runs yield different results? |
| Verify convergence of the training algorithm. | (1) Examine the slope of final loss values across replications. (2) Visually check the convergence of key quantities for selected seeds. | Will training the model for additional epochs lead to a practically relevant improvement in performance or a reduction in total loss? |
| Verify accurate learning of expert data. | Visually compare model-implied and expert-elicited statistics. | Was the method successful in accurately capturing the expert data? |
| Evaluation Stage | | |
| Examine the learned priors across the different seeds | Visually inspect the marginal priors and correlations between model parameters. | How much do the learned priors vary between different seeds? Were any degenerate prior distributions learned? Do we observe any form of multi-modality? Can any of the learned priors be ruled out as unreasonable post hoc? |
| Obtain the final learned prior for subsequent analysis. | Perform model averaging using weights based on relative loss performance. | Instead of selecting a single prior, compute a model average over practically equivalent priors to account for additional variability due to non-identifiability. |

Table 3 Overview of the analysis workflow used in the simulation studies.

computing the corresponding true-elicited statistics. The *true* joint prior is defined by independent normal distributions for each model parameter: $\beta_0 \sim \text{Normal}(0.1, 0.1)$ and $\beta_1 \sim \text{Normal}(-0.1, 0.3)$.

To assess the *informativeness* of the selected set of elicited statistics, we conduct a sensitivity analysis, with the results shown in Figure 3. In each row, a single hyperparameter is varied across the range shown on the x-axis, while all other hyperparameters are held constant at their true values, indicated by the red vertical line. The columns present the two elicited statistics, specifically the five quantiles (in shades of blue and green) for $y \mid x_0$ and $y \mid x_1$. The horizontal gray line is included for reference, with the upper two rows indicating results for the intercept parameter β_0 and the lower two rows for the slope parameter β_1 . The results of the sensitivity analysis indicate that the selected elicited statistics provide sufficient informativeness for the model hyperparameters.

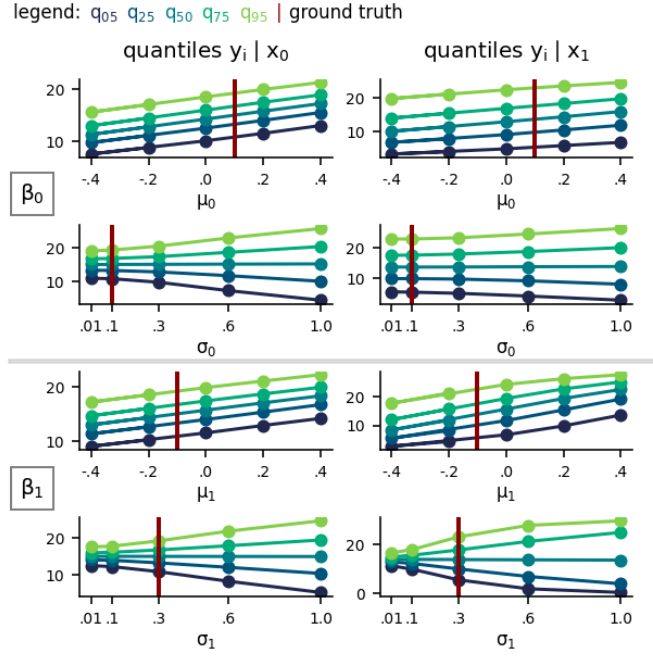


Fig. 3 *Binomial model—Sensitivity Analysis*: Rows represent hyperparameters of each model parameter. Columns represent elicited statistics: five quantiles for $y | x_0$ and $y | x_1$. Quantiles are depicted in different colors. In each row, the corresponding hyperparameter, is varied across the range shown on the x-axis, while all other hyperparameters are held constant at their true values, indicated by the red vertical line. The horizontal gray line is included for reference, with the upper two rows indicating results for the intercept parameter β_0 and the lower two rows for the slope parameter β_1 .

Fitting Stage

We ran the training algorithm 30 times with different random seeds and conducted an initial convergence check by inspecting the slope of the last 100 epochs for each replication. In Figure 4, the upper row shows the absolute slope (scaled by a factor of 100) for each replication. In the lower row, the learning trajectory of the total loss is shown for the best-performing (leftmost) and the four worst-performing replications. We observe a near-zero slope for the best model, indicating convergence, while the negative slopes for the worst-performing seeds suggest that the learning algorithm continues to make progress. However, a visual inspection of the learning trajectories for the four worst-performing replications, exemplified in Figure 5 for seed 11, indicates satisfactory convergence for all quantities of interest. This includes the total loss, the individual loss components (upper row), as well as the means and standard deviations of the marginal priors (lower row). Therefore, although there appears to be minor ongoing learning progress, the results will only change very minimally. Overall, we conclude that the training process was successful.

The corresponding final learned elicited statistics for each replication are shown in the first two plots in Figure 6. Each true quantile (x-axis) is plotted against its corresponding learned quantile (y-axis) for each replication. Points that align perfectly

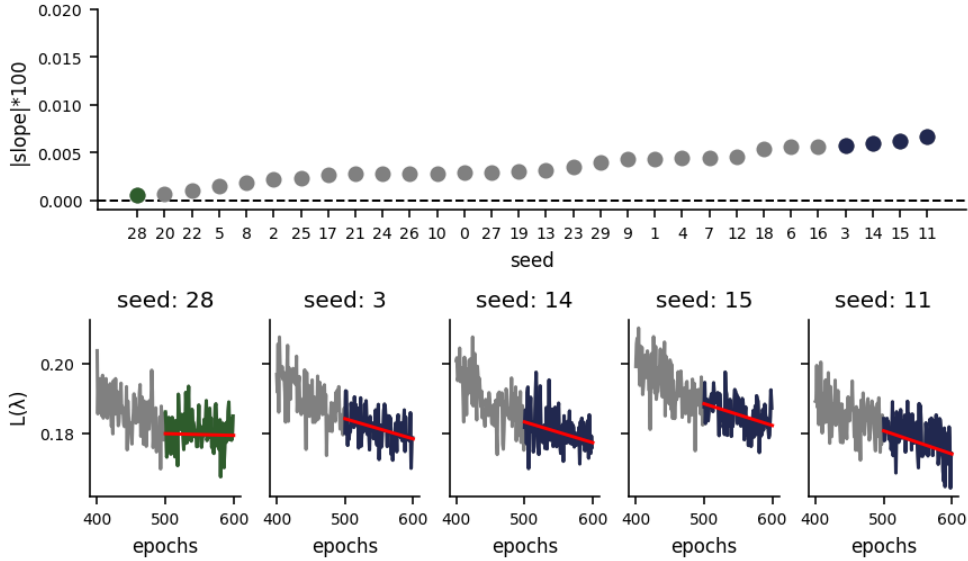


Fig. 4 *Binomial model—Preliminary convergence check for all 30 replications*: The upper plot displays the absolute slope of the total loss trajectory (scaled by a factor of 100) over the last 100 epochs on the y-axis, with each replication shown along the x-axis. The replications (i.e., seeds) are arranged in ascending order based on the magnitude of the absolute slope. The best-performing model, with an almost zero slope, is seed 28, while the worst-performing models, indicated by negative slopes, are seeds 3, 14, 15, and 11. The lower plot illustrates the loss trajectories of the best- and worst-performing seeds over the last 200 epochs. The loss updates for the final 100 epochs are highlighted in green for the best model and in blue for the worst models, with a red line segment indicating the respective slope.

with the diagonal dashed line represent a perfect match between true and learned quantiles. Points above the diagonal indicate that the learned quantiles are higher than the true ones (and vice versa for lower points). Additionally, in the rightmost plot in Figure 6, we present the true (red) and learned (orange) correlations between the marginal priors. Consistent with successful convergence, the elicited statistics, including the correlations, are accurately learned across all replications.

Evaluation Stage

Finally, we can examine the prior distribution learned by each of the 30 replications. Figure 7b displays the learned marginal priors for each replication in grey. Since all priors closely align with the ground truth (indicated by the dotted black line), the different seeds are visually indistinguishable. These results suggest that the set of elicited statistics provides sufficient information to practically identify model M1. This conclusion is further supported by the weights used for model averaging, depicted in Figure 7a. The weights represent the relative performance of each replication based on their total loss (see Section 2.5 for details). All replications perform equally well, resulting in a uniform weighting scheme. The corresponding model average is depicted

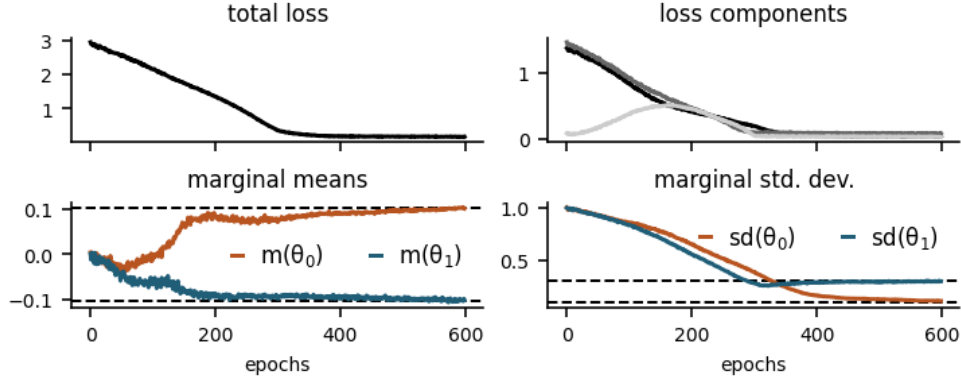


Fig. 5 *Binomial model—Visual convergence check for seed=11*: The plots display the updating trajectory across epochs for various quantities of interest: the total loss (upper left), individual loss components (upper right), and the mean and standard deviation of the marginal priors (lower left and lower right, respectively).

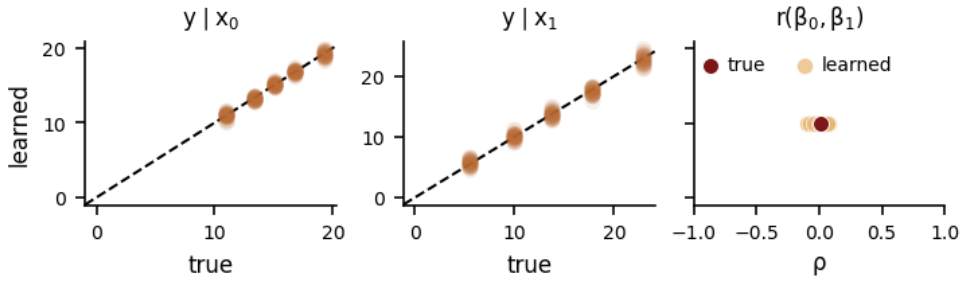


Fig. 6 *Binomial model—Learned elicited statistics for all 30 replications*: The two leftmost plots show the learned quantiles (y-axis) vs. the true quantiles (x-axis) of each replication for the two target quantities, $y | x_0$ and $y | x_1$. The diagonal line serves as a reference, where points lying on the line indicate a perfect match between learned and true quantiles. The rightmost plot displays the learned (orange) vs. true (red) correlations. Given that we assume independence between model parameters in this scenario, the true correlation is zero. Consistent with convergence, all learned elicited statistics closely match the ground truth.

via a dashed black line in Figure 7b. In this example, all learned marginal priors, the ground truth, and the model average coincide, showcasing an ideal scenario.

4.3 Simulation Studies 2: Normal Likelihood

In the remaining simulation studies, we aim to evaluate the method’s performance using a model with increased complexity, specifically a normal regression model with standard deviation σ and mean μ_i , where μ_i depends on a three-level grouping variable

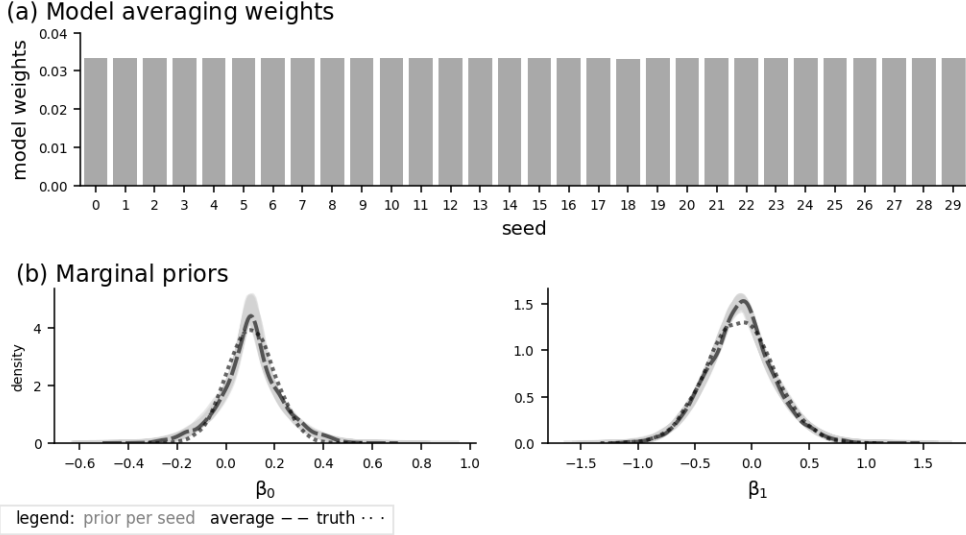


Fig. 7 *Binomial model—Learned marginal priors for all 30 replications:* (a) Computed weights per replication used for model averaging, reflecting the relative performance of each model based on the final total loss. In this scenario, all replications perform equally well, resulting in uniform weights. (b) The learned marginal priors for each replication are shown in grey. The dotted black line represents the ground truth and the dashed, black line indicates the model average. In this case, the elicited statistics are sufficiently informative to practically identify the generative model, leading the learned priors, the ground truth, and the model average to coincide.

encoded via the dummy variables x_1 and x_2 :

$$\begin{aligned}
 y_i &\sim \text{Normal}(\mu_i, \sigma) \\
 \mu_i &= \beta_0 + \beta_1 x_{1,i} + \beta_2 x_{2,i} \\
 \beta_0, \beta_1, \beta_2, \sigma &\sim p_\lambda(\beta_0, \beta_1, \beta_2, \sigma) \\
 \theta &\equiv (\beta_0, \beta_1, \beta_2, \sigma)
 \end{aligned}$$

with β_0 , β_1 , and β_2 being the regression coefficients representing the intercept and the two group contrasts, respectively. The goal is to learn a joint prior for the model parameters θ . To systematically assess our method, we use the same model across all upcoming simulation studies, varying only the *true* joint prior in each scenario:

- **Scenario 1 (M2):** Independent normal priors for the regression coefficients are defined as $\beta_0 \sim \text{Normal}(10, 2.5)$, $\beta_1 \sim \text{Normal}(7, 1.3)$, $\beta_2 \sim \text{Normal}(2.5, 0.8)$, with a Gamma prior for the random noise, $\sigma \sim \text{Gamma}(5, 2)$
- **Scenario 2 (M3):** This setup is identical to M2 but introduces skewed normal priors for β_1 and β_2 , where $\beta_1 \sim \text{SkewNormal}(7, 1.3, 4)$ ¹ and $\beta_2 \sim \text{SkewNormal}(2.5, 0.8, 4)$.

¹For the skewed normal distribution, we use the implementation from TensorFlow Probability (Abadi et al 2016), which features the two-piece normal distribution (Fernández and Steel 1998). This distribution is parameterized by location, scale, and shape parameters. The shape parameter controls the skewness, with values above one resulting in a right-skewed distribution.

- **Scenario 3 (M4):** This scenario introduces a dependency structure among the model coefficients β using a correlated multivariate normal distribution, with marginal distributions identical to those in M2. All other aspects remain the same as in M2. The correlated prior is specified as:

$$\beta \sim \text{Mv-Normal} \left(\begin{bmatrix} 10 \\ 7 \\ 2.5 \end{bmatrix}, D(s) \mathbf{R} D(s) \right) \quad \text{with}$$

$$\mathbf{R} = \begin{bmatrix} 1. & 0.3 & -0.3 \\ 0.3 & 1. & -0.2 \\ -0.3 & -0.2 & 1. \end{bmatrix}, \quad s = (2.5, 1.3, 0.8)$$

where \mathbf{R} denotes the correlation matrix and s the vector of standard deviations.

4.3.1 Scenario 1: Independent Normal Priors

Setup & Elicitation Stage

We begin with a brief assessment of the selected elicited statistics, with sensitivity analysis results detailed in Appendix A.2. While the intercept coefficient, β_0 , is well-informed by all three target quantities related to the predictive distributions of the groups, the slope coefficients, β_1 and β_2 , are each informed by only one target quantity, specifically those corresponding to group 2 and group 3, respectively. Consequently, we anticipate greater difficulty in accurately learning these coefficients. Additionally, we included R^2 among the target quantities to aid the learning algorithm in distinguishing parameter uncertainty from data uncertainty. However, given the limited data available, we expect considerable variability in the learned model variances.

Fitting Stage

To verify successful convergence, we first examined the absolute slopes across all 30 replications, followed by a detailed visual inspection of the learning trajectories for the loss components and additional quantities of interest in the replications with the highest absolute slopes (see Appendix A.2 for results). Based on this analysis, we conclude that the learning process was successful. The corresponding learned model-implied statistics are shown in Figure 8 and demonstrate a strong match between the learned and true elicited statistics.

Evaluation Stage

The corresponding learned marginal priors of each replication are depicted in Figure 9. Figure 9a displays the distribution of the computed weights used for model averaging. The replication with the highest weight is highlighted in green, while the replication with the lowest weight is highlighted in orange. In Figure 9b, the learned marginal priors of each replication are depicted in grey. The dotted black line refers to the ground truth and the dashed black line to the model average. Additionally, the marginal priors for the best- and worst-performing replications are highlighted in their respective colors. The results suggest that the elicited statistics provide sufficient information to

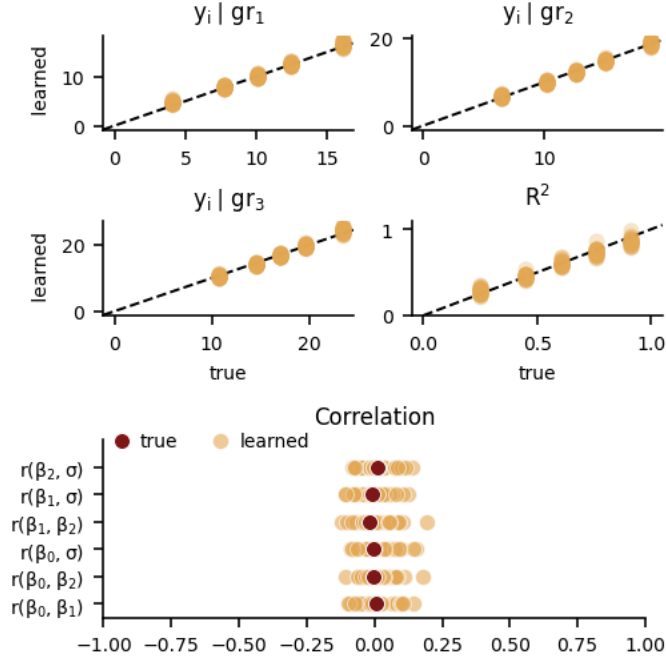


Fig. 8 *Normal model / Scenario 1 (M2)* — Learned elicited statistics for all 30 replications: Upper plots show the learned quantiles (y -axis) vs. the true quantiles (x -axis) of each replication for the four target quantities $y \mid gr_i$ with $i = 1, 2, 3$ and R^2 . The diagonal line serves as a reference, where points lying on the line indicate a perfect match between learned and true quantiles. The lower plot displays the learned (orange) vs. true (red) correlations between the model parameters. Given the independence assumption, the true correlation is zero. All learned elicited statistics closely match the ground truth.

accurately learn the marginal prior of β_0 . In contrast, the remaining learned marginal priors display substantial variation. Notably, for σ , most replications yield a marginal prior concentrated around the mean of a Gamma(5, 2) distribution. This indicates that, while the elicited statistics capture some information about the average level of data variation, they convey limited information about its uncertainty. However, despite the variability in the learned marginal priors, there is no degenerate or otherwise highly outlying distribution whose plausibility we would exclude *a priori*.

4.3.2 Scenario 2: Skewed Normal Priors

Setup & Elicitation Stage

This scenario differs from the previous one only in the ground truth, where we introduce a skew-normal marginal prior for the two slope coefficients, β_1 and β_2 . However, since we use the same set of "elicited" statistics, the sensitivity analysis (see Appendix A.3) already suggests that there is likely insufficient information to disentangle the variance and skewness components for these two slope coefficients; therefore, these components are most likely not identified.

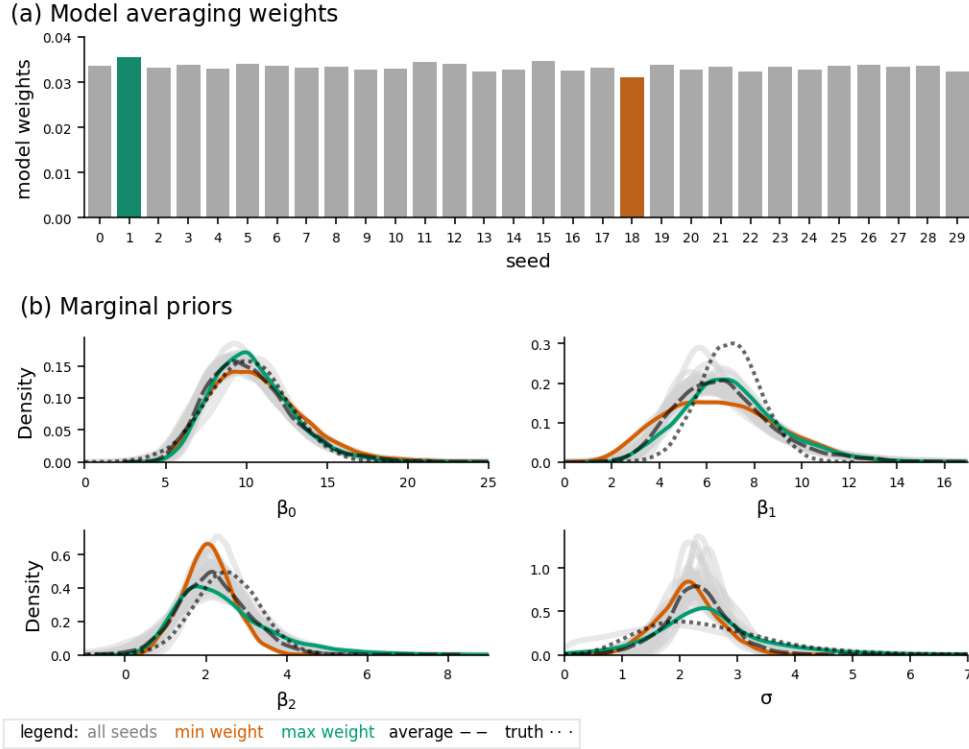


Fig. 9 Normal model / Scenario 1 ($M2$) — Learned marginal priors for all 30 replications: (a) Computed weights per replication used for model averaging, reflecting the relative performance of each model based on the final total loss. The highest and lowest weights are highlighted in green and orange, respectively. (b) The learned marginal priors for each replication are shown in grey, with the dotted black line representing the ground truth and the dashed black line indicating the model average. The marginals for the seeds with the highest and lowest weights are respectively colored. Although the elicited statistics provide sufficient information to accurately learn the prior for β_0 , the substantial variation in the learned priors for the other model parameters indicates a certain lack of model identification.

Fitting Stage

The convergence diagnostics are depicted in Appendix A.3 and indicate successful convergence. The corresponding match between the model-implied and true “elicited” statistics is shown in Figure 10. We observe a good alignment for both the correlations and the quantiles of the predictive distributions across the three groups, $y \mid gr_i$ with $i = 1, 2, 3$. However, for the quantiles of R^2 , there is some difficulty in accurately capturing the true elicited statistics. Specifically, the learned quantiles of R^2 tend

to be overestimated, which implies that σ tend to be underestimated². This general tendency appears to be particularly pronounced for one specific replication.

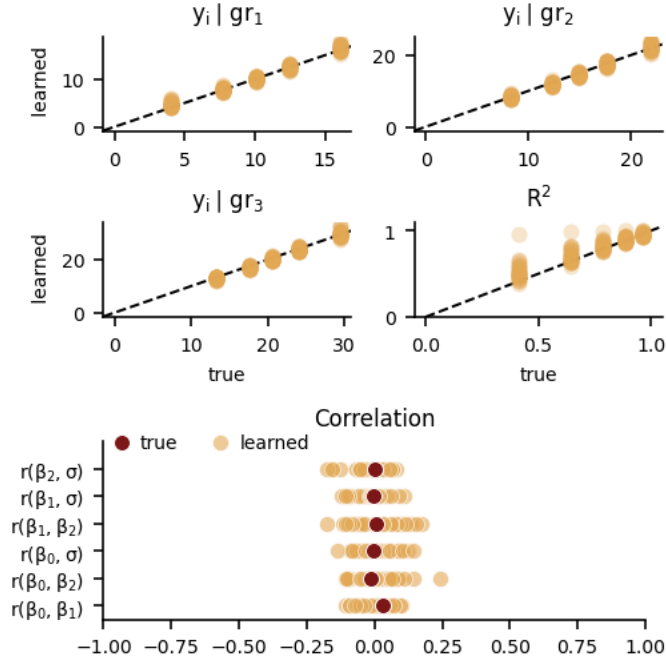


Fig. 10 Normal model / Scenario 2 (M3) — Learned elicited statistics for all 30 replications: Upper plots show the learned quantiles (y-axis) vs. the true quantiles (x-axis) of each replication for the four target quantities $y | gr_i$ with $i = 1, 2, 3$ and R^2 . The diagonal line serves as a reference, where points lying on the line indicate a perfect match between learned and true quantiles. The lower plot displays the learned (orange) vs. true (red) correlations between the model parameters. Given the independence assumption, the true correlation is zero. All learned elicited statistics closely match the ground truth, except for R^2 , where the learned quantiles tend to be overestimated, implying an underestimation of σ (see text for details).

Evaluation Stage

Indeed, when examining the learned marginal priors in Figure 10b, we see that for σ , there is one replication that places a significant amount of prior mass on values near zero. This replication corresponds to the seed with the smallest weight as depicted in Figure 10a and is therefore highlighted in orange. The next step in this case would be to consult with the domain expert on the plausibility of the learned marginal priors, particularly considering whether the marginal prior for σ , with values close to zero, is meaningful in the context of the study. Since σ shares the same scale as the outcome

² R^2 is defined as the ratio of the variance of the predictive mean to the total variance. Consequently, the variance components of the coefficients (σ_0, σ_1 , and σ_2) contribute to the numerator, while the denominator includes these components along with σ . Therefore, an increase in R^2 implies a decrease in σ , which then yields in a reduction of the denominator relative to the numerator.

variable y , it allows for an assessment of how much or how little noise in the data is considered realistic. This situation illustrates how, even if a domain expert may not have been able to express precise expectations for σ initially, the resulting distributions can enable them to retrospectively rule out certain cases they find unrealistic.

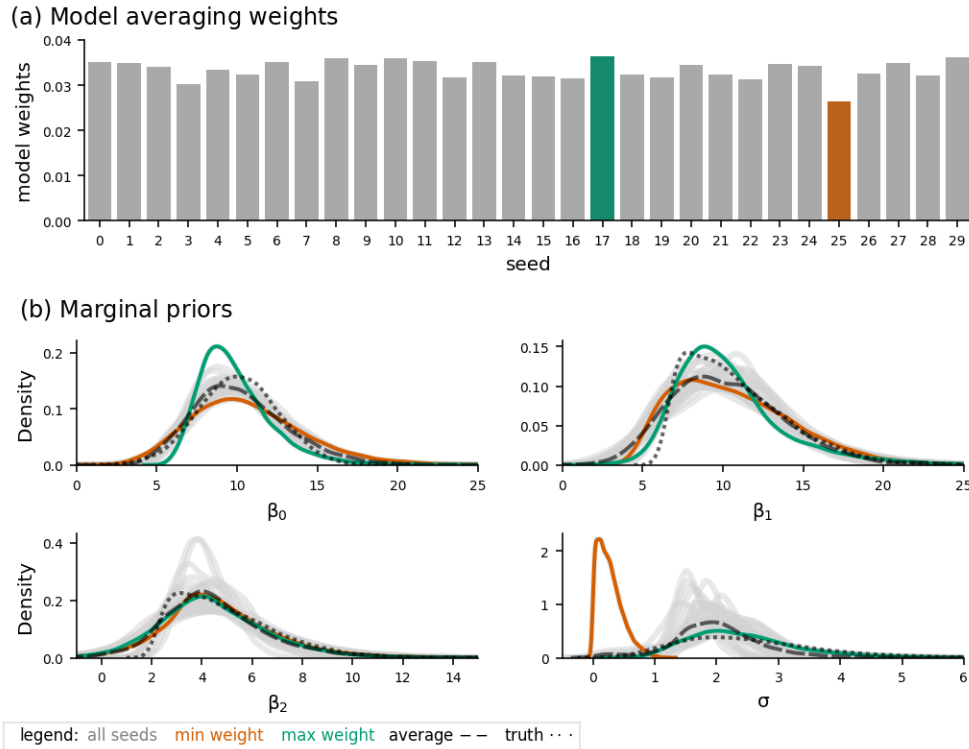


Fig. 11 *Normal model / Scenario 2 (M3) — Learned marginal priors for all 30 replications:* (a) Computed weights per replication used for model averaging, reflecting the relative performance of each model based on the final total loss. The highest and lowest weights are highlighted in green and orange, respectively. (b) The learned marginal priors for each replication are shown in grey, with the dotted black line representing the ground truth and the dashed black line the model average. The marginals for the seeds with the highest and lowest weights are highlighted in the respective colors. Substantial variation in the learned priors for all model parameters suggests a lack of model identification. However, no degenerate distribution is learned. For σ , the learned priors exhibit some degree of multi-modality, with one replication in particular placing a significant amount of probability mass on small values of σ .

4.3.3 Scenario 3: Correlated Normal Priors

Setup & Elicitation Stage

In this final scenario, we introduced a specific dependency structure among the regression coefficients, while all other aspects remained identical to Scenario 1 (M2). The

results of the sensitivity analysis, provided in Appendix A.4, indicate that the current set of “elicited” statistics would not provide sufficient information to learn the dependency structure. To address this, we included the pairwise correlations between model parameters as input to the learning algorithm. As a result, the correlation should be accurately learned, given the full information provided.

Fitting Stage

The convergence check indicated successful convergence, with results provided in Appendix A.4. The corresponding match between the model-implied and true “elicited” statistics is shown in Figure 12. We observe a close match for the quantiles of the predictive distribution of each group, while, as noted already in Scenario 2, the quantiles for R^2 remain more challenging to learn accurately. However, in this scenario, the overestimation of R^2 is less pronounced, occurring in only one replication, while all other replications appear to learn this statistic accurately. The correlation plot (shown on the bottom of Figure 12) also demonstrates good learning of the dependency information. Therefore, with the provided correlation information, the learning algorithm is able to learn a correlated joint prior.

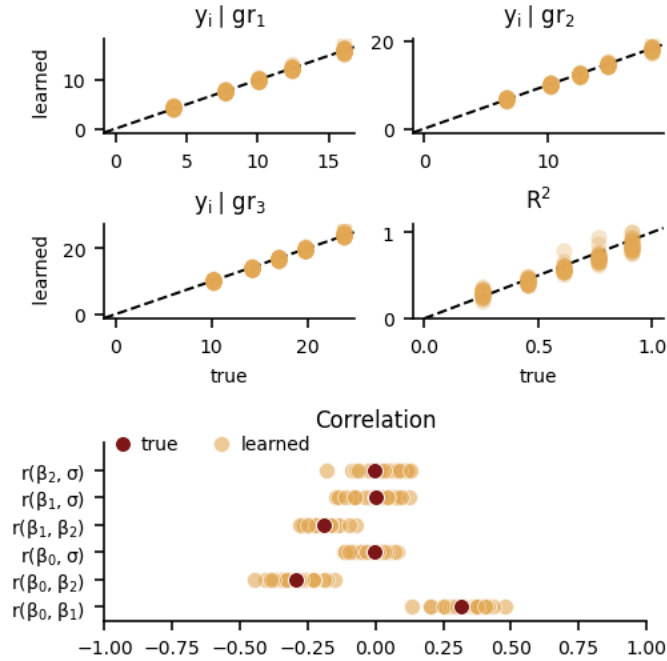


Fig. 12 Normal model / Scenario 3 (M_4) — Learned elicited statistics for all 30 replications: Upper plots show the learned quantiles (y-axis) vs. the true quantiles (x-axis) of each replication for the four target quantities $y | gr_i$ with $i = 1, 2, 3$ and R^2 . The diagonal line serves as a reference, where points lying on the line indicate a perfect match between learned and true quantiles. The lower plot displays the learned (orange) vs. true (red) correlations between the model parameters. All learned elicited statistics match the ground truth, with some variation observed between replications.

Evaluation Stage

In Figure 13b, the learned marginal priors for each replication are shown, with the computed weights used for model averaging displayed in Figure 13a. As expected, the learned marginal priors for the intercept parameter, β_0 , show little variation, while there is substantial variation in the learned marginal priors for the other model parameters, whereby the variation for β_1 is less pronounced compared to β_2 . As previously noted through the elicited statistics, there is again one replication that learns a marginal prior for σ that places significantly more probability mass on values near zero compared to the learned marginal priors of the other replications. These results again suggest some multi-modality in the learned priors, which could be useful for constraining the search space if certain sets of priors are deemed unrealistic by the domain expert.

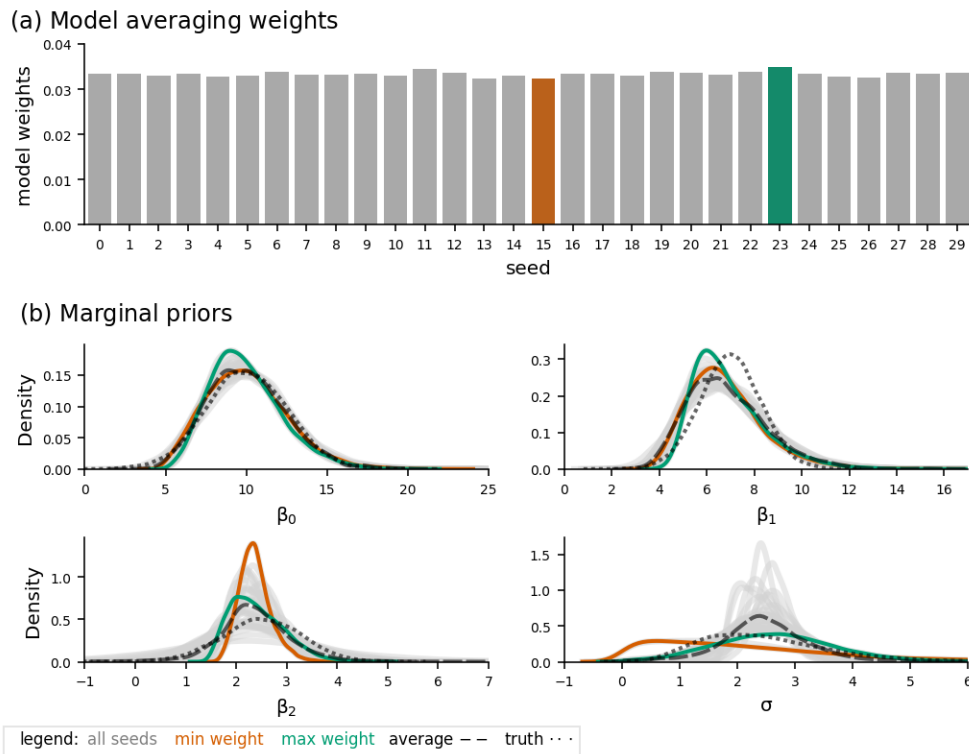


Fig. 13 Normal model / Scenario 3 (M_4) — Learned marginal priors for all 30 replications: (a) Computed weights per replication used for model averaging, reflecting the relative performance of each model based on the final total loss. The highest and lowest weights are highlighted in green and orange, respectively. (b) The learned marginal priors for each replication are shown in grey, with the dotted black line representing the ground truth and the dashed black line the model average. The marginals for the seeds with the highest and lowest weights are highlighted in the respective colors.

5 Discussion & Outlook

In this paper, we introduce an elicitation method for learning *non-parametric joint priors* building on and extending our simulation-based framework (Bockting et al 2024). This work demonstrates that our framework is capable of supporting the development of various elicitation methods, in addition to the previously introduced method for learning independent parametric priors. To learn non-parametric joint priors, we utilize normalizing flows (Kobyzev et al 2020) to learn flexible joint priors for the model parameters. Through four simulation studies, we demonstrated the successful learning of such priors informed by expert knowledge. Although we employ normalizing flows in this work, other generative models, such as flow matching (Lipman et al 2022) or diffusion models (Cao et al 2024) are also compatible with our framework and can be readily used as a drop-in replacement.

We view the ability to use the same framework for implementing various types of elicitation methods advantageous. By constructing these methods from shared modules (building blocks), our approach not only facilitates direct comparison between elicitation methods but also supports the establishment of benchmarks within the field. Furthermore, a unified framework facilitates the development of a standardized set of diagnostics and analysis tools, addressing a gap that currently exists in this area (Mikkola et al 2023). These tools can be employed during the elicitation process to specify target quantities, choose appropriate elicitation techniques, and evaluate the learned prior distributions.

Within our framework, *expert knowledge* can be specified in various ways—ranging from querying model parameters to observable quantities or any derived statistic—tailored to the specific problem and the expertise of the domain expert being queried. This flexibility is achieved through the inclusion of a module that defines both the quantities to be elicited from the expert (cf. target quantities) and the techniques used to query these quantities (cf. elicitation techniques). This design choice provides users with maximum flexibility in specifying the set of quantities to be elicited from the domain expert. However, it also places the responsibility on the user to define a valid and appropriate set of quantities to query from the expert (Simpson et al 2017). We would argue that this is in general a desirable property of a method, as it avoids imposing specific modeling choices on the user. Instead of requiring that the problem is framed in a predefined way, the method allows users to adapt it to their specific needs (Regenwetter and Cavagnaro 2019; Simpson et al 2017; Scott 2017). However, in practice, this flexibility is only effective if good recommendations, guidelines, and diagnostics are available to help users define an appropriate set of quantities to query from the expert (Garthwaite et al 2013).

A significant challenge in this context is assessing whether the chosen set of statistics is *sufficiently informative* for the corresponding model. The goal is not necessarily to identify a unique prior that fully defines the generative model. Instead, the aim is to determine a set of equivalently plausible priors, which is theoretically justified since a domain expert is unlikely to have a single “true” prior in mind (Winkler 1967). This introduces at least two additional requirements for an elicitation method. First, it should include an efficient implementation that allows the training algorithm to be executed multiple times with different seeds, enabling the assessment of variability in

the learned prior distributions. Second, the elicitation method should ideally offer additional diagnostics or advanced techniques, such as model selection or model averaging, to assist the user (Falconer et al 2022). In this work, we propose a model averaging method in which the weights calculated for averaging can also serve as diagnostics, helping to identify potential outliers within the set of learned priors. Identifying these edge cases could provide a valuable starting point for evaluating the plausibility of the learned priors in collaboration with a domain expert.

If the set of learned prior distributions includes degenerate cases, this signals the need for additional constraints. These constraints could involve eliciting further or alternative quantities (i.e., elicited statistics) from the expert and/or adding a regularization term to the total loss function to better guide the learning process. To evaluate the informativeness of the elicited statistics, we use a sensitivity analysis as a preliminary evaluation tool (O’Hagan and Oakley 2004). Additionally, we advocate for employing an oracle (i.e., simulating data from a known ground truth) and conducting multiple training replications with varying random seeds. These strategies provide a solid initial check to determine if the learned priors require further constraints. Overall, this discussion highlights the importance of developing comprehensive tutorials and resources to guide users effectively through the elicitation workflow as a key task for future work.

Another important direction for future work is the development of a technique that can learn the *dependency structure* of a joint prior while simultaneously querying the expert about interpretable quantities. In this paper, we demonstrated that our method can learn a joint prior with the corresponding dependency structure when informed with the pairwise model parameter correlation. However, for practical applicability, the goal is to build on these results and develop a method that infers the correlation indirectly from the expert by asking about interpretable quantities. Recently, Mikkola et al (2024) proposed a method that uses pairwise comparisons or ranking techniques to learn a multivariate prior density, which could serve as an interesting avenue for future research.

Other important design choices within our framework that require appropriate default settings include the specification of the discrepancy measure and the selection of the optimization approach, among other aspects. So far, in all simulation studies, we have used the maximum mean discrepancy (MMD, Gretton et al 2006) to evaluate the discrepancy between the model-implied and expert-elicited statistics. The only exception is the correlation information, for which we employed an L2 loss. One key advantage of the MMD is its flexibility in handling a wide range of statistics, from simple point estimates to complex histogram data. However, a notable limitation of the MMD is its high (i.e., quadratic) computational cost. In contrast, the L2 loss is computationally efficient but lacks the capability to process histogram data. Despite the higher computational cost, the MMD consistently showed very good performance and robustness across all simulation studies so far. Therefore, it appears to be a solid choice as a default discrepancy measure. Future work should study the performance of different loss functions depending on different elicited statistics, with the goal to develop user guidelines for selecting an appropriate loss function.

Furthermore, in all simulation studies conducted so far, we used mini-batch SGD to optimize the prior network parameters. Given the generally good performance observed, we believe that this optimization method is a solid default choice. However, we aim to explore additional optimization approaches within our framework, such as Bayesian optimization (as employed by [Manderson and Goudie \(2023\)](#)). Comparing these approaches in terms of performance and the level of hyperparameter tuning required could offer valuable insights into the conditions under which optimization method might be more advantageous than the other.

Declarations

Acknowledgements

We thank Dmytro Perepolkin and Luna Fazio for their valuable comments and suggestions that greatly improved the manuscript. All authors gratefully acknowledge the computing time provided on the Linux HPC cluster at Technical University Dortmund (LiDO3), partially funded in the course of the Large-Scale Equipment Initiative by the Deutsche Forschungsgemeinschaft (DFG, German Research Foundation) as project 271512359.

Funding

Not applicable.

Competing interests

The authors have no competing interests to declare that are relevant to the content of this article.

Consent to participate

Not applicable.

Consent for publication

Not applicable.

Data availability

The simulation results are available at <https://osf.io/xrzh6/>.

Materials availability

Not applicable.

Code availability

A Python package, including code to simulate, analyse and plot data, is available at https://github.com/florence-bocking/prior_elicitation/tree/main/elicit/manuscript_non_parametric_joint_prior

Author contribution

Conceptualization: PB, SR, FB, Methodology: PB, FB, Software: FB, Writing (Original Draft): FB, Writing (Review & Editing): SR, PB, Visualization: FB, Supervision: PB, Funding acquisition: PB, SR

References

- Abadi M, Barham P, Chen J, et al (2016) TensorFlow: A system for large-scale machine learning. In: 12th USENIX symposium on operating systems design and implementation (OSDI 16), pp 265–283, <https://doi.org/10.5555/3026877.3026899>
- Authority EFS (2014) Guidance on expert knowledge elicitation in food and feed safety risk assessment. *EFSA J.* 12(6):3734. <https://doi.org/10.2903/j.efsa.2014.3734>
- Betancourt M (2020) Towards a principled bayesian workflow. Blog Post, URL https://betanalpha.github.io/assets/case_studies/principled_bayesian_workflow.html
- Bischof R, Kraus M (2021) Multi-objective loss balancing for physics-informed deep learning. arXiv preprint <https://doi.org/10.48550/arXiv.2110.09813>
- Bissiri PG, Holmes CC, Walker SG (2016) A general framework for updating belief distributions. *J. R. Stat. Soc. Series. B Stat. Methodol.* 78(5):1103–1130. <https://doi.org/10.1111/rssb.12158>
- Bockting F, Radev ST, Bürkner PC (2024) Simulation-based prior knowledge elicitation for parametric bayesian models. *Sci. Rep.* 14(1):17330. <https://doi.org/10.1038/s41598-024-68090-7>
- Bond-Taylor S, Leach A, Long Y, et al (2021) Deep generative modelling: A comparative review of vaes, gans, normalizing flows, energy-based and autoregressive models. *IEEE Trans. Pattern Anal. Mach. Intell.* 44(11):7327–7347. <https://doi.org/10.1109/TPAMI.2021.3116668>
- Buckland ST, Burnham KP, Augustin NH (1997) Model selection: an integral part of inference. *Biometrics* pp 603–618. <https://doi.org/10.2307/2533961>
- Cao H, Tan C, Gao Z, et al (2024) A survey on generative diffusion models. *IEEE Trans. Knowl. Data Eng.* 36(7):2814–2830. <https://doi.org/10.1109/TKDE.2024.3361474>
- Claeskens G, Hjort NL (2008) Model selection and model averaging. Cambridge books
- Clemen RT, Fischer GW, Winkler RL (2000) Assessing dependence: Some experimental results. *Manage. Sci.* 46(8):1100–1115. <https://doi.org/10.1287/mnsc.46.8.1100.12023>
- Cooke RM (1991) Experts in uncertainty: opinion and subjective probability in science. Oxford University Press, USA
- Crawshaw M (2020) Multi-task learning with deep neural networks: A survey. arXiv preprint <https://doi.org/10.48550/arXiv.2009.09796>

- Crowder M (1992) Bayesian priors based on a parameter transformation using the distribution function. *Ann. Inst. Stat. Math.* 44:405–416. <https://doi.org/10.1007/BF00050695>
- Denham R, Mengersen K (2007) Geographically assisted elicitation of expert opinion for regression models. *Bayesian Anal.* 2(1):99–136. <https://doi.org/10.1214/07-BA205>
- Depaoli S, Winter SD, Visser M (2020) The importance of prior sensitivity analysis in bayesian statistics: demonstrations using an interactive shiny app. *Front. Psychol.* 11:608045. <https://doi.org/10.3389/fpsyg.2020.608045>
- Dickey J, Lindley DV, Press SJ (1985) Bayesian estimation of the dispersion matrix of a multivariate normal distribution. *Commun. Stat. Theory Methods* 14(5):1019–1034. <https://doi.org/10.1080/03610928508828960>
- Dillon JV, Langmore I, Tran D, et al (2017) Tensorflow distributions. arXiv preprint <https://doi.org/10.48550/arXiv.1711.10604>
- Dinh L, Krueger D, Bengio Y (2014) Nice: Non-linear independent components estimation. In: ICLR Workshop, <https://doi.org/10.48550/arXiv.1410.8516>
- Dinh L, Sohl-Dickstein J, Bengio S (2016) Density estimation using real nvp. arXiv preprint <https://doi.org/10.48550/arXiv.1605.08803>
- Draxler F, Wahl S, Schnörr C, et al (2024) On the universality of coupling-based normalizing flows. arXiv preprint <https://doi.org/10.48550/arXiv.2402.06578>
- Durkan C, Bekasov A, Murray I, et al (2019) Neural spline flows. *Adv. Neural. Inf. Process. Syst.* 32. <https://doi.org/10.5555/3454287.3454962>
- Falconer JR, Frank E, Polaschek DL, et al (2022) Methods for eliciting informative prior distributions: A critical review. *Decis. Anal.* 19(3):189–204. <https://doi.org/10.1287/deca.2022.0451>
- Fernández C, Steel MF (1998) On bayesian modeling of fat tails and skewness. *J. Am. Stat. Assoc.* 93(441):359–371. <https://doi.org/10.2307/2669632>
- Feydy J, Séjourné T, Vialard FX, et al (2019) Interpolating between optimal transport and mmd using sinkhorn divergences. In: The 22nd International Conference on Artificial Intelligence and Statistics, PMLR, pp 2681–2690, URL <https://proceedings.mlr.press/v89/feydy19a.html>
- Figurnov M, Mohamed S, Mnih A (2018) Implicit reparameterization gradients. *Adv. Neural. Inf. Process. Syst.* 31. <https://doi.org/10.5555/3326943.3326984>
- Gabry J, Simpson D, Vehtari A, et al (2019) Visualization in bayesian workflow. *J. R. Stat. Soc. Ser. A Stat. Soc.* 182(2):389–402. <https://doi.org/10.1111/rssa.12378>

- Garthwaite PH, Kadane JB, O’Hagan A (2005) Statistical methods for eliciting probability distributions. *J. Am. Stat. Assoc.* 100(470):680–701. <https://doi.org/10.1198/016214505000000105>
- Garthwaite PH, Al-Awadhi SA, Elfadaly FG, et al (2013) Prior distribution elicitation for generalized linear and piecewise-linear models. *J. Appl. Stat.* 40(1):59–75. <https://doi.org/10.1080/02664763.2012.734794>
- Gelman A, Simpson D, Betancourt M (2017) The prior can often only be understood in the context of the likelihood. *Entropy* 19(10):555. <https://doi.org/10.3390/e19100555>
- Gelman A, Goodrich B, Gabry J, et al (2019) R-squared for bayesian regression models. *Am. Stat.* pp 307–309. <https://doi.org/10.1080/00031305.2018.1549100>
- Gelman A, Vehtari A, Simpson D, et al (2020) Bayesian workflow. arXiv preprint <https://doi.org/10.48550/arXiv.2011.01808>
- Gokhale D, Press SJ (1982) Assessment of a prior distribution for the correlation coefficient in a bivariate normal distribution. *J. R. Stat. Soc. Ser. A Stat. Soc.* 145(2):237–249. <https://doi.org/10.2307/2981537>
- Goodfellow I, Bengio Y, Courville A (2016) Deep learning. MIT press
- Gosling JP (2018) Shelf: the sheffield elicitation framework. *Elicitation: The science and art of structuring judgement* pp 61–93
- Gretton A, Borgwardt K, Rasch M, et al (2006) A kernel method for the two-sample-problem. *Adv. Neural. Inf. Process. Syst.* 19. <https://doi.org/10.5555/2976456.2976521>
- Harris CR, Millman KJ, van der Walt SJ, et al (2020) Array programming with NumPy. *Nature* 585(7825):357–362. <https://doi.org/10.1038/s41586-020-2649-2>
- Hartmann M, Agiashvili G, Bürkner P, et al (2020) Flexible prior elicitation via the prior predictive distribution. In: Peters J, Sontag D (eds) *Proc.Conf.UAI, PMLR*, pp 1129–1138, URL <https://proceedings.mlr.press/v124/hartmann20a.html>
- Johnson SR, Tomlinson GA, Hawker GA, et al (2010) Methods to elicit beliefs for Bayesian priors: a systematic review. *J. Clin. Epidemiol.* 63(4):355–369. <https://doi.org/10.1016/j.jclinepi.2009.06.003>
- Kadane J, Wolfson LJ (1998) Experiences in elicitation. *Statistician* 47(1):3–19. <https://doi.org/10.1111/1467-9884.00113>
- Kadane JB, Dickey JM, Winkler RL, et al (1980) Interactive elicitation of opinion for a normal linear model. *J. Am. Stat. Assoc.* 75(372):845–854. <https://doi.org/10.1080/01621459.1980.10477562>

- Kingma DP, Dhariwal P (2018) Glow: Generative flow with invertible 1x1 convolutions. *Advances in neural information processing systems* 31
- Kingma DP, Welling M (2014) Auto-encoding variational bayes. *stat* 1050:1. <https://doi.org/10.48550/arXiv.1312.6114>
- Kobyzev I, Prince SJ, Brubaker MA (2020) Normalizing flows: An introduction and review of current methods. *IEEE Trans. Pattern Anal. Mach. Intell.* 43(11):3964–3979. <https://doi.org/10.1109/TPAMI.2020.2992934>
- Lipman Y, Chen RT, Ben-Hamu H, et al (2022) Flow matching for generative modeling. *arXiv preprint* <https://doi.org/10.48550/arXiv.2210.02747>
- Liu S, Johns E, Davison AJ (2019) End-to-end multi-task learning with attention. In: *Proceedings of the IEEE/CVF conference on computer vision and pattern recognition*, pp 1871–1880, <https://doi.org/10.1109/CVPR.2019.00197>
- Manderson AA, Goudie RJ (2023) Translating predictive distributions into informative priors. *arXiv preprint* <https://doi.org/10.48550/arXiv.2303.08528>
- Martin TG, Burgman MA, Fidler F, et al (2012) Eliciting expert knowledge in conservation science. *Conserv. Biol.* 26(1):29–38. <https://doi.org/10.1111/j.1523-1739.2011.01806.x>
- McKinney W, et al (2010) Data structures for statistical computing in python. In: *Proceedings of the 9th Python in Science Conference*, Austin, TX, pp 51–56, <https://doi.org/10.25080/Majora-92bf1922-00a>
- Mikkola P, Martin OA, Chandramouli S, et al (2023) Prior knowledge elicitation: The past, present, and future. *Bayesian Anal.* 1(1):1–33. <https://doi.org/10.1214/23-BA1381>
- Mikkola P, Acerbi L, Klami A (2024) Preferential normalizing flows. *arXiv preprint* <https://doi.org/10.48550/arXiv.2410.08710>
- Morris DE, Oakley JE, Crowe JA (2014) A web-based tool for eliciting probability distributions from experts. *Environ. Model. Softw.* 52:1–4. <https://doi.org/10.1016/j.envsoft.2013.10.010>
- Nemani V, Biggio L, Huan X, et al (2023) Uncertainty quantification in machine learning for engineering design and health prognostics: A tutorial. *Mech. Syst. Signal Process.* 205:110796. <https://doi.org/10.1016/j.ymsp.2023.110796>
- Oakley JE, O’Hagan A (2007) Uncertainty in prior elicitation: a nonparametric approach. *Biometrika* 94(2):427–441. <https://doi.org/10.1093/biomet/asm031>
- O’Hagan A, Oakley JE (2004) Probability is perfect, but we can’t elicit it perfectly. *Reliab. Eng. Syst. Saf.* 85(1-3):239–248. <https://doi.org/10.1016/j.res.2004.03.014>

- O'Hagan A, Buck CE, Daneshkhah A, et al (2006) Uncertain judgements: eliciting experts' probabilities. John Wiley & Sons
- O'Hagan A (2019) Expert knowledge elicitation: subjective but scientific. *Am. Stat.* 73(sup1):69–81. <https://doi.org/10.1080/00031305.2018.1518265>
- Papamakarios G, Nalisnick E, Rezende DJ, et al (2021) Normalizing flows for probabilistic modeling and inference. *J. Mach. Learn.* 22(57):1–64. URL <http://jmlr.org/papers/v22/19-1028.html>
- Perepolkin D, Lindsröm E, Sahlin U (2023) Quantile-parameterized distributions for expert knowledge elicitation. OSF preprint <https://doi.org/10.31219/osf.io/tq3an>
- Perepolkin D, Goodrich B, Sahlin U (2024) Hybrid elicitation and quantile-parametrized likelihood. *Stat. Comput.* 34(1):11. <https://doi.org/10.1007/s11222-023-10325-0>
- Peterson C, Miller A (1964) Mode, median, and mean as optimal strategies. *J. Exp. Psychol.* 68(4):363. <https://doi.org/10.1037/h0040387>
- Radev ST, Mertens UK, Voss A, et al (2020) Bayesflow: Learning complex stochastic models with invertible neural networks. *IEEE Trans. Neural. Netw. Learn. Syst.* 33(4):1452–1466. <https://doi.org/10.1109/TNNLS.2020.3042395>
- Radev ST, Schmitt M, Schumacher L, et al (2023) Bayesflow: Amortized bayesian workflows with neural networks. *J. Open Source Softw.* 8(89):5702. <https://doi.org/https://doi.org/10.21105/joss.05702>
- Regenwetter M, Cavagnaro DR (2019) Tutorial on removing the shackles of regression analysis: How to stay true to your theory of binary response probabilities. *Psychol. methods* 24(2):135. <https://doi.org/10.1037/met0000196>
- Igorzata Roos M, Martins TG, Held L, et al (2015) Sensitivity analysis for bayesian hierarchical models. *Bayesian Anal.* 10(2):321–349. <https://doi.org/10.1214/14-BA909>
- Scott JG (2017) Prior specification is engineering, not mathematics. *Stat. Sci.* 32(1):29–32. <https://doi.org/10.1214/16-STS576>
- da Silva EdS, Kuśmierczyk T, Hartmann M, et al (2019) Prior specification via prior predictive matching: Poisson matrix factorization and beyond. Preprint at <https://doi.org/10.48550/arXiv.1910.12263>
- Simpson D, Rue H, Riebler A, et al (2017) Penalising model component complexity: A principled, practical approach to constructing priors. *Stat. Sci.* 32(1):1–28. <https://doi.org/10.1214/16-STS576>

- Stefan AM, Evans NJ, Wagenmakers EJ (2022) Practical challenges and methodological flexibility in prior elicitation. *Psychol. Methods* 27(2):177–197. <https://doi.org/10.1037/met0000354>
- Van Dongen S (2006) Prior specification in bayesian statistics: three cautionary tales. *J. Theor. Biol.* 242(1):90–100. <https://doi.org/10.1016/j.jtbi.2006.02.002>
- Wagenmakers EJ, Farrell S (2004) AIC model selection using akaike weights. *Psychon. Bull. Rev.* 11:192–196. <https://doi.org/10.3758/BF03206482>
- Wang L, Ng AH, Deb K (2011) *Multi-objective evolutionary optimisation for product design and manufacturing*. Springer
- Winkler RL (1967) The assessment of prior distributions in bayesian analysis. *J. Am. Stat. Assoc.* 62(319):776–800. <https://doi.org/10.1080/01621459.1967.10500894>

Appendix A Simulation Studies

A.1 Training time

The average training time across the 30 replications was

- **Binomial model:** 24 minutes and 10 seconds (± 33 seconds).
- **Independent normal scenario:** 66 minutes and 50 seconds (± 5 min: 53 secs).
- **Skewed normal scenario:** 74 minutes and 34 seconds (± 9 min: 16 secs).
- **Correlated normal scenario:** 73 minutes and 18 seconds (± 1 min: 59 secs).

A.2 Independent normal scenario

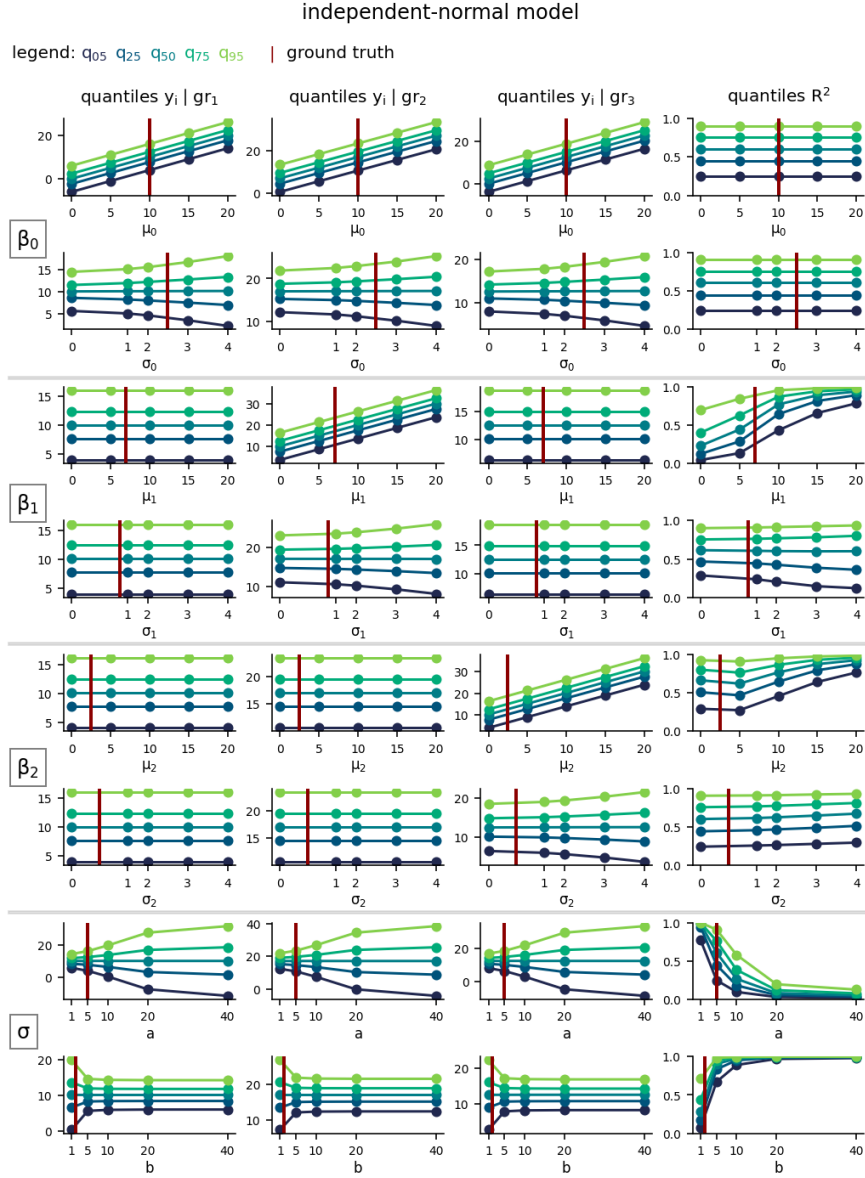


Fig. A1 Normal model / Scenario 1 ($M2$) — Sensitivity Analysis: Rows represent hyperparameters of each model parameter. Columns represent elicited statistics: five quantiles for $y | gr_i$ with $i = 1, 2, 3$ and for R^2 . Quantiles are depicted in different colors. In each row, the corresponding hyperparameter, is varied across the range shown on the x-axis, while all other hyperparameters are held constant at their true values, indicated by the red vertical line. The horizontal gray line is included as a reference to distinguish between the different model parameters.

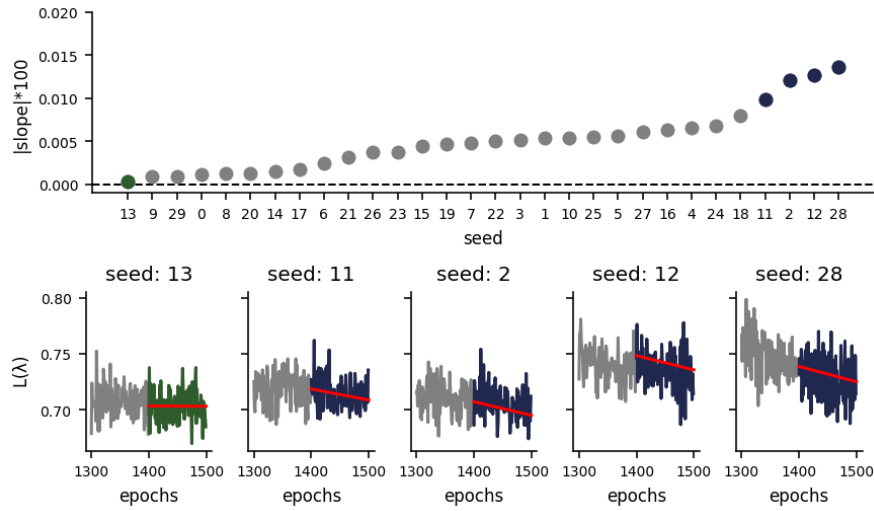
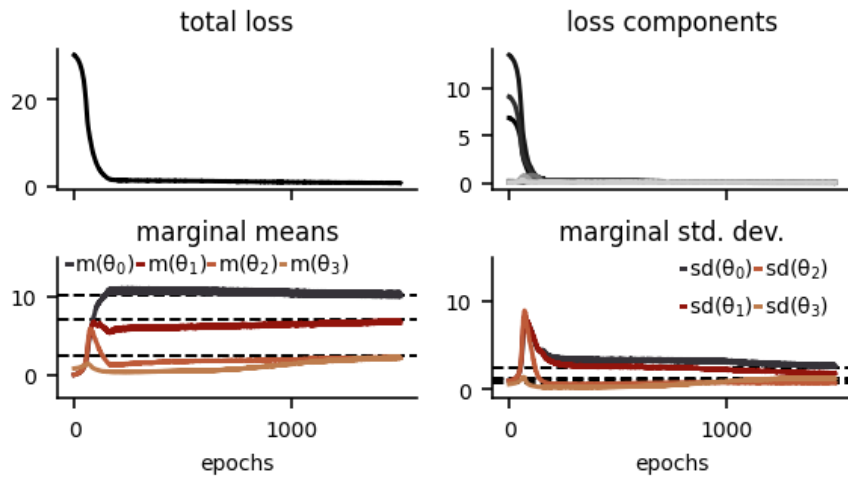


Fig. A2 *Normal model / Scenario 1 (M2) — Preliminary Convergence Check for all 30 replications:* The upper plot displays the absolute slope of the total loss trajectory (scaled by a factor of 100) over the last 100 epochs on the y-axis, with each replication shown along the x-axis. The replications (i.e., seeds) are arranged in ascending order based on the magnitude of the absolute slope. The best-performing model, with an almost zero slope, is seed 13, while the worst-performing models, indicated by negative slopes, are seeds 11, 2, 12, and 28. The lower plot illustrates the loss trajectories of the best- and worst-performing seeds over the last 200 epochs. The loss updates for the final 100 epochs are highlighted in green for the best model and in blue for the worst models, with a red line segment indicating the respective slope.

(a) Convergence diagnostics (seed: 28)



(b) Joint prior distribution (seed: 28)

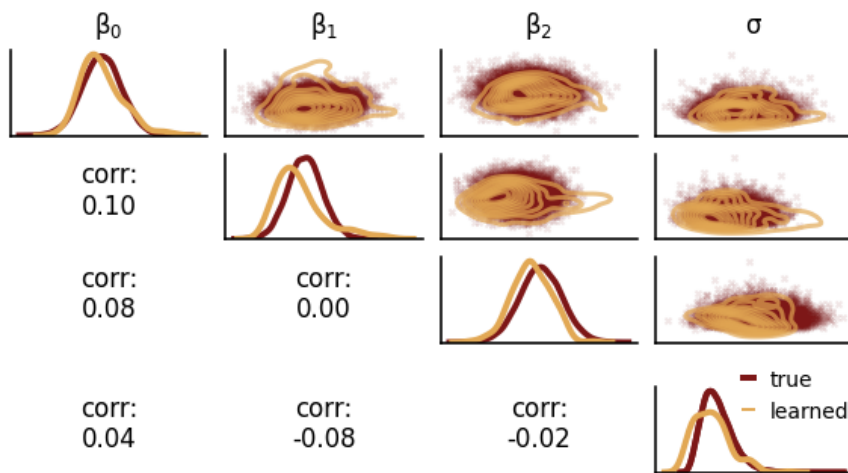


Fig. A3 Normal model / Scenario 1 ($M2$) — Visual convergence check for seed=28: (a) Updating trajectory across epochs for various quantities of interest: the total loss (upper left), individual loss components (upper right), and the mean and standard deviation of the marginal priors (lower left and lower right, respectively). (b) Learned joint prior with marginal distributions along the diagonal and correlation information in the off-diagonal.

A.3 Skewed normal scenario

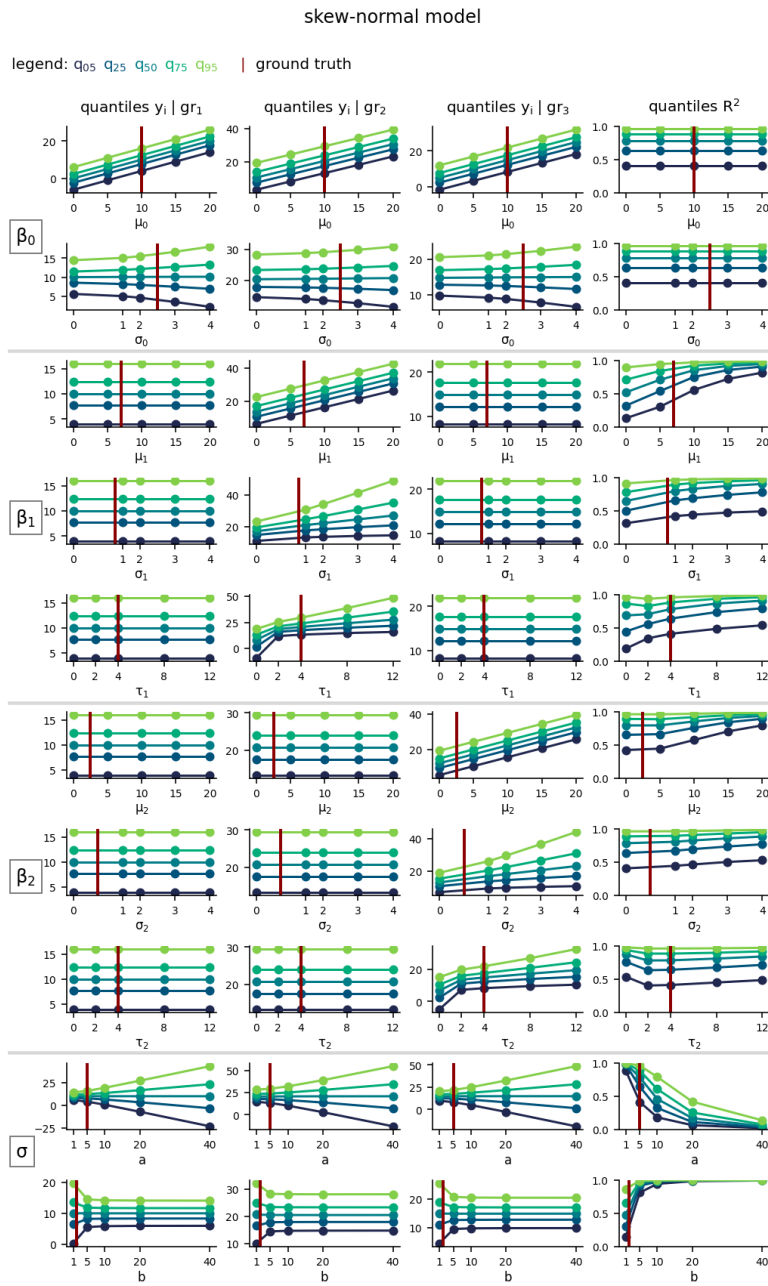


Fig. A4 Normal model / Scenario 2 (M3) — Sensitivity Analysis: Rows represent hyperparameters of each model parameter. Columns represent elicited statistics: five quantiles for $y | gr_i$ with $i = 1, 2, 3$ and for R^2 . Quantiles are depicted in different colors. In each row, the corresponding hyperparameter, is varied across the range shown on the x-axis, while all other hyperparameters are held constant at their true values, indicated by the red vertical line. The horizontal gray line is included as a reference to distinguish between the different model parameters.

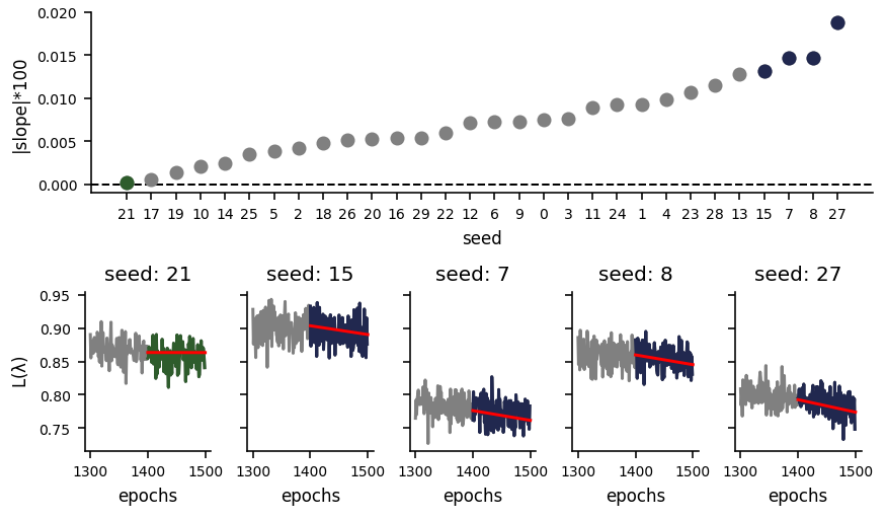
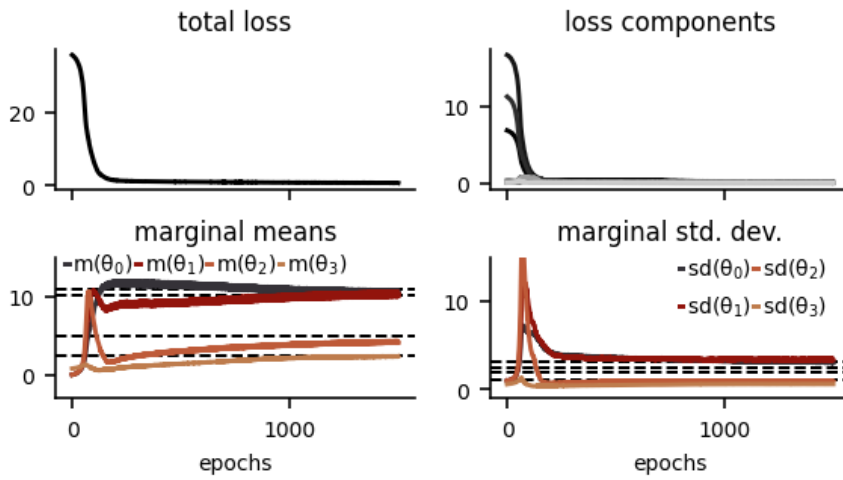


Fig. A5 *Normal model / Scenario 2 (M3) — Preliminary Convergence Check for all 30 replications:* The upper plot displays the absolute slope of the total loss trajectory (scaled by a factor of 100) over the last 100 epochs on the y-axis, with each replication shown along the x-axis. The replications (i.e., seeds) are arranged in ascending order based on the magnitude of the absolute slope. The best-performing model, with an almost zero slope, is seed 21, while the worst-performing models, indicated by negative slopes, are seeds 15, 7, 8, and 27. The lower plot illustrates the loss trajectories of the best- and worst-performing seeds over the last 200 epochs. The loss updates for the final 100 epochs are highlighted in green for the best model and in blue for the worst models, with a red line segment indicating the respective slope.

(a) Convergence diagnostics (seed: 27)



(b) Joint prior distribution (seed: 27)

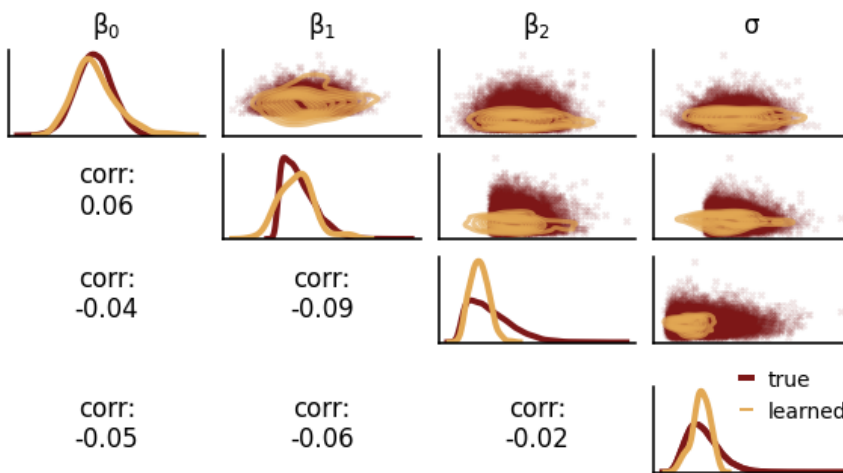


Fig. A6 Normal model / Scenario 2 (M3) — Visual convergence check for seed=27: (a) Updating trajectory across epochs for various quantities of interest: the total loss (upper left), individual loss components (upper right), and the mean and standard deviation of the marginal priors (lower left and lower right, respectively). (b) Learned joint prior with marginal distributions along the diagonal and correlation information in the off-diagonal.

A.4 Correlated normal scenario

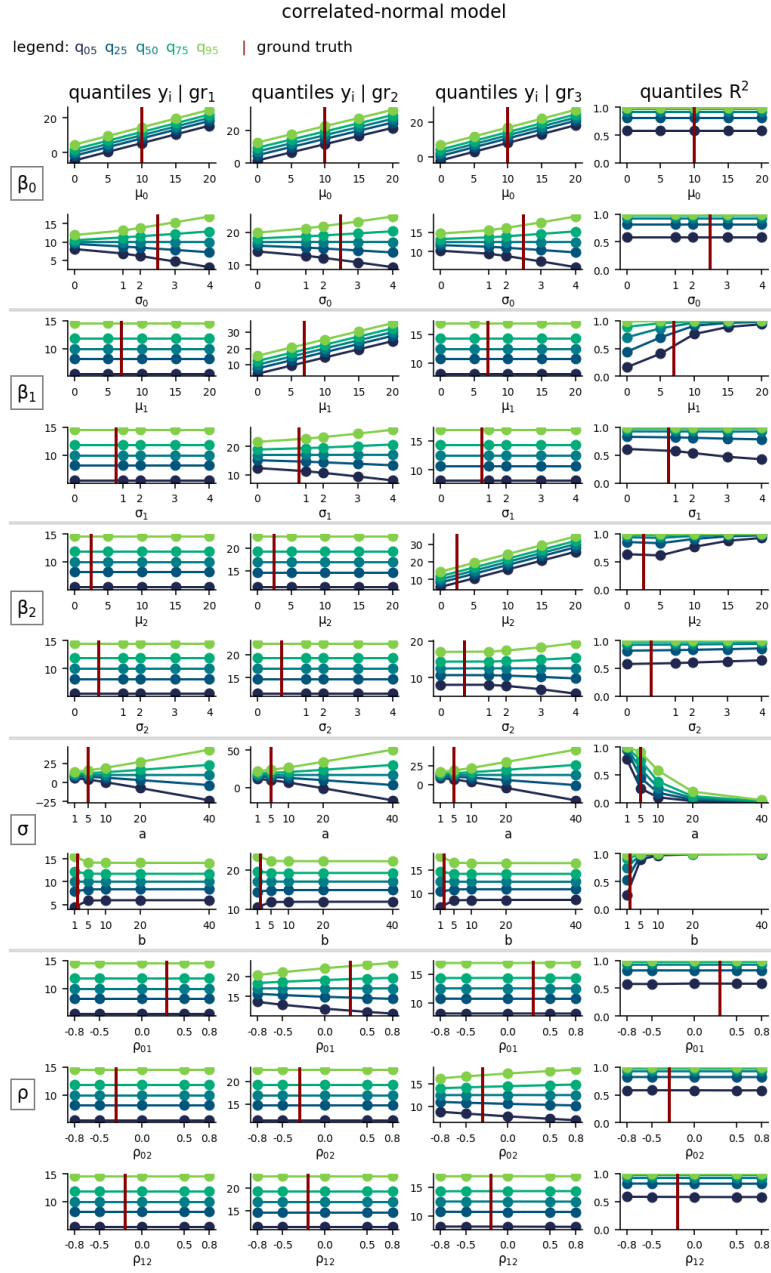


Fig. A7 Normal model / Scenario 3 (M_4) — Sensitivity Analysis: Rows represent hyperparameters of each model parameter. Columns represent elicited statistics: five quantiles for $y | gr_i$ with $i = 1, 2, 3$ and for R^2 . Quantiles are depicted in different colors. In each row, the corresponding hyperparameter, is varied across the range shown on the x-axis, while all other hyperparameters are held constant at their true values, indicated by the red vertical line. The horizontal gray line is included as a reference to distinguish between the different model parameters.

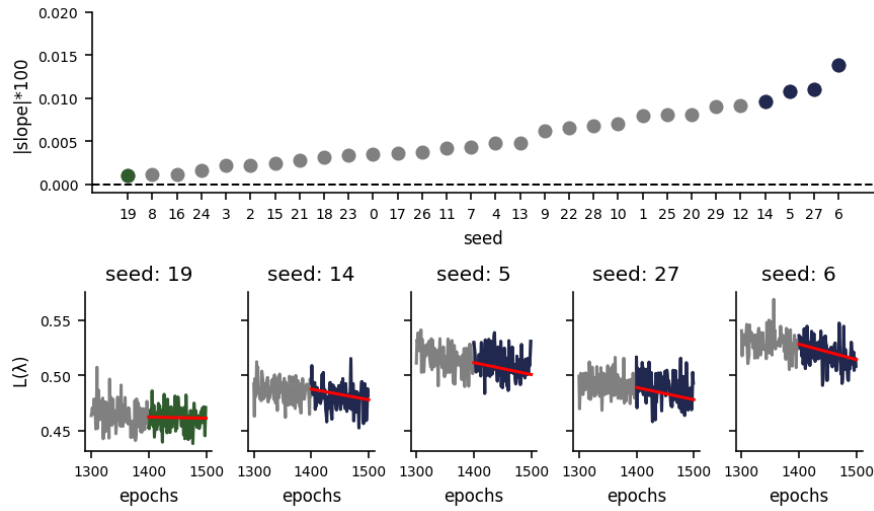
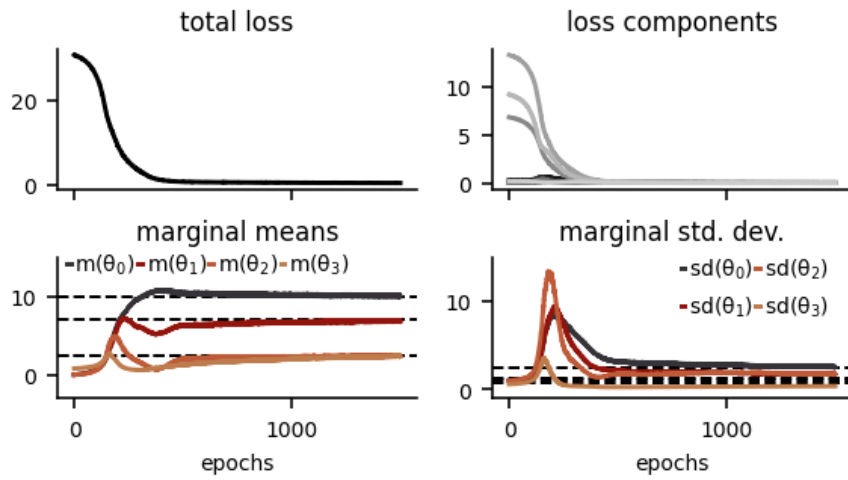


Fig. A8 *Normal model / Scenario 3 (M_4) — Preliminary Convergence Check for all 30 replications:* The upper plot displays the absolute slope of the total loss trajectory (scaled by a factor of 100) over the last 100 epochs on the y-axis, with each replication shown along the x-axis. The replications (i.e., seeds) are arranged in ascending order based on the magnitude of the absolute slope. The best-performing model, with an almost zero slope, is seed 19, while the worst-performing models, indicated by negative slopes, are seeds 14, 5, 27, and 6. The lower plot illustrates the loss trajectories of the best- and worst-performing seeds over the last 200 epochs. The loss updates for the final 100 epochs are highlighted in green for the best model and in blue for the worst models, with a red line segment indicating the respective slope.

(a) Convergence diagnostics (seed: 6)



(b) Joint prior distribution (seed: 6)

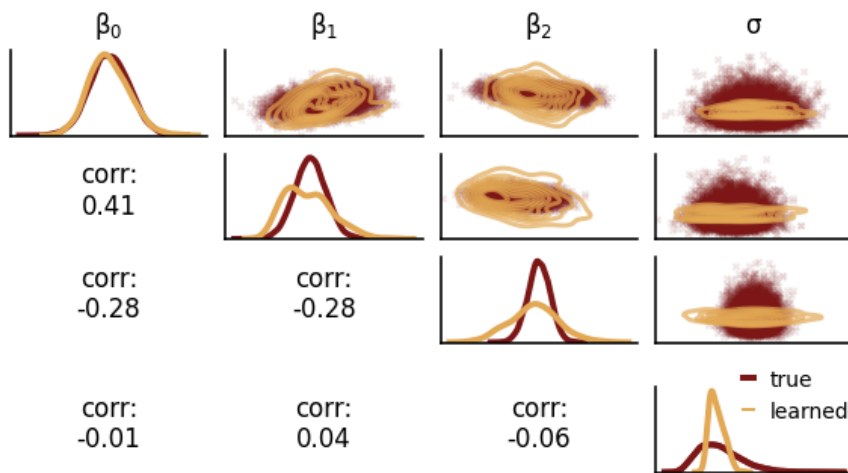


Fig. A9 Normal model / Scenario 3 (M_4) — Visual convergence check for seed=26: (a) Updating trajectory across epochs for various quantities of interest: the total loss (upper left), individual loss components (upper right), and the mean and standard deviation of the marginal priors (lower left and lower right, respectively). (b) Learned joint prior with marginal distributions along the diagonal and correlation information in the off-diagonal.